

# Chapter 7. Bay-Delta SELFE Calibration Overview

## 7.1 Introduction

The Delta Modeling Section at DWR and Virginia Institute of Marine Sciences recently concluded a collaborative initial calibration of the 3-D semi-implicit Eulerian-Lagrangian finite element (SELFE) hydrodynamic model for the Bay-Delta (Figure 7-1). This chapter describes the scope of the calibration, assumptions, and additions made for the domain, preliminary calibration results, and discussion of suitability of the model for various types of studies. A more technically comprehensive calibration document is in preparation.

The goal of our project is to develop an open-source, cross-scale multidimensional model suitable to answer flow and water quality questions involving large extents on the Bay-Delta system over periods of several years. Target applications include:

- Habitat creation and conveyance options under BDCP alternatives
- Salinity intrusion changes under drought or sea level rise
- Velocity changes in nearby channels following the installation of barriers
- Fate of mercury produced in the Liberty Island complex in the north Delta
- Temperature, flow, and food production in the estuary as part of a 3-model full life cycle bioenergetic model of salmon (as participants in the NOAA SESAME project).

These applications vary a great deal in scope. Some can be studied with our base model as-is using a few quick adjustments, but the last two require focal regions of intense study, multi-disciplinary biogeochemistry, or more careful validation of a particular transport mechanism. In our collaboration with NOAA and NASA in the SESAME project, the flexibility and openness of SELFE allowed swift incorporation of CoSINE, an alternate nutrient model to the standard EcoSIM 2.0 in SELFE emphasizing the most important constituents for salmon in the system.

Our immediate goal has been to establish a foundation – to develop a sense of global accuracy, requiring that we resolve (or craftily under-resolve) the main mechanisms of hydrodynamics and transport up the estuary and in Delta channels. These include gravitational circulation and exchange flow, periodic stratification, tidal trapping, flood-ebb asymmetry of flow paths, shear dispersion, primary flow streamlines, and perhaps some secondary circulation in large channels. Although we expect our calibration to continue to improve, further work will be continue in project-dependent directions. Due to its flexible mesh, the model is easily re-usable in a near field/far field arrangement whereby the base model provides a pre-calibrated background grid for an extension or focal region of study.

Our base calibration focuses on hydrodynamics and salinity transport and on the North Bay and Delta. The reasons for concentrating on salt as a first step are well-known. Salinity intrusion is the most important water quality issue facing the water projects. Salinity (conductivity) is extensively monitored at stations throughout the estuary. Second, in the stratified part of the estuary, salt is essential to the vertical structure of flow through density – so modeling salinity is prerequisite to modeling the transport of other constituents such as sediment and organisms that are preferentially distributed vertically in the water

column. Finally, in much of the estuary and Delta, salt does behave much like any other diffuse, conservative tracer, and inasmuch as all conservative constituents are equivalent, a good salinity calibration is a good conservative tracer calibration.

## 7.2 SELFE Model

SELFE is a cross-scale 3-D (optionally 2-D) shallow water open source hydrodynamic model jointly developed by the Center for Coastal Margin Observation and Prediction (CMOP) and Virginia Institute of Marine Sciences. In the past, SELFE has been coupled to several ecological and water quality modules, two wind-wave interaction models, 2-D and 3-D sediment transport, data assimilation, and oil spill applications. A number of these are available as open source modules. In the current project, we have tackled some of the practicalities of Bay-Delta modeling, including the incorporation of subgrid hydraulic structures such as radial gates, weirs, and culverts.

The underlying computational engine in SELFE is a second-generation semi-implicit model sharing some of the algorithmic background of the UnTRIM family of models, which also includes UnTRIM and SUNTANS and emerging models from Deltares and FVCOM. The semi-implicit approach is robust, efficient, sufficiently accurate, and offers a natural treatment of wetting and drying. SELFE's predecessor, ELCIRC, was perhaps the first open source model of this class to receive wide distribution and that prior experience figured heavily into our model selection decision. SELFE shares some code with ELCIRC, but its discretization and solution scheme includes innovations to the algorithm that improves the depiction of bathymetry and salinity plume transport. SELFE has also been parallelized and used by groups all over the world on a diverse variety of high performance computers.

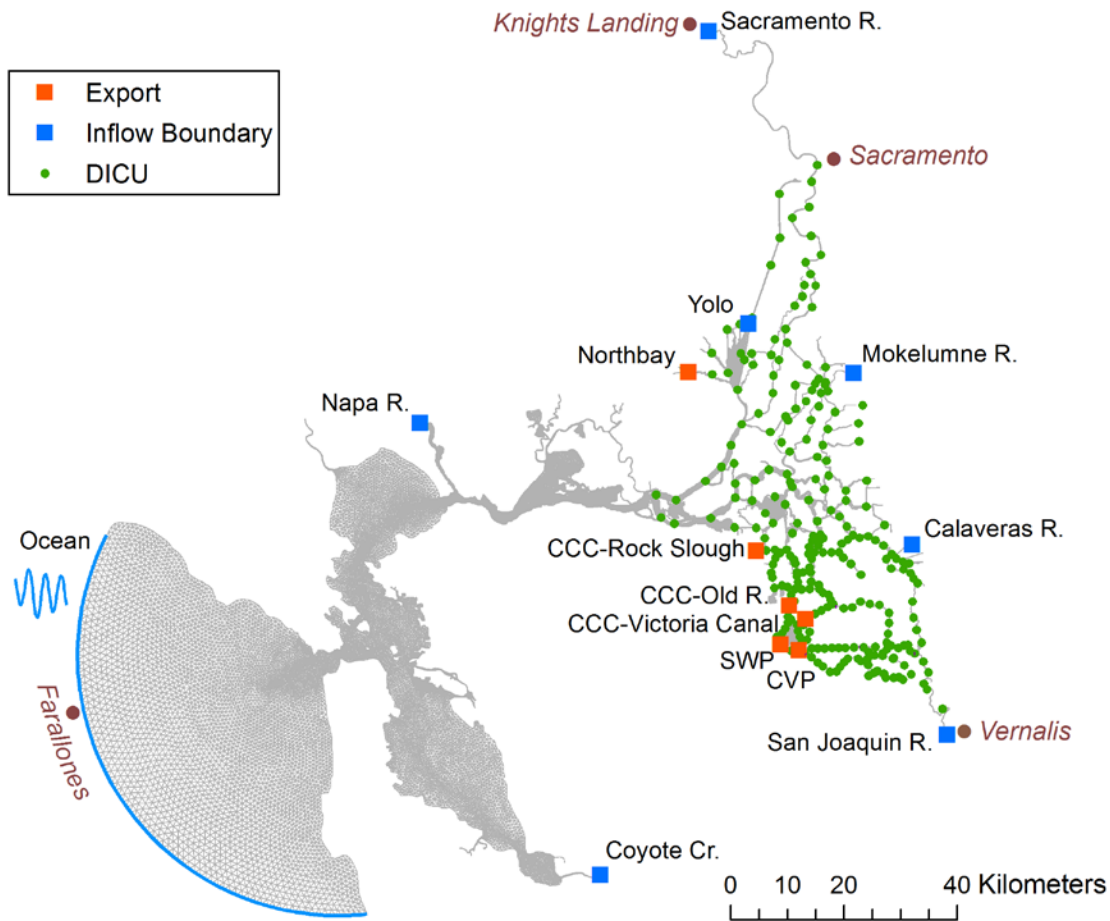
### 7.2.1 Formulation

The formulation of SELFE is based on classic expressions of mass and momentum conservation within a shallow fluid, as well as the transport equations for salt and heat. Flow is assumed to be *Reynolds averaged*, which means that small scale turbulent mixing of momentum and dissolved constituents is not resolved directly, but rather tied to mean flow properties using a turbulence closure. Pressure in the model is assumed to be hydrostatic in our application. SELFE has a non-hydrostatic module, but non-hydrostatic modeling requires higher resolution in space and time than an estuary-scale solution can typically provide in long-term simulations.

The main variables calculated by SELFE are the elevation of the free surface (stage), three-dimensional velocity and concentrations of salinity, temperature, and other scalar concentrations (only salinity is considered in this calibration), as well as turbulent quantities. Extensions in the SELFE suite use the flow field to calculate particle trajectories, sediment transport, and nutrient availability. The input required by SELFE includes the initial state of the system and boundary time series representing fluxes and/or water surfaces at all the open boundaries.

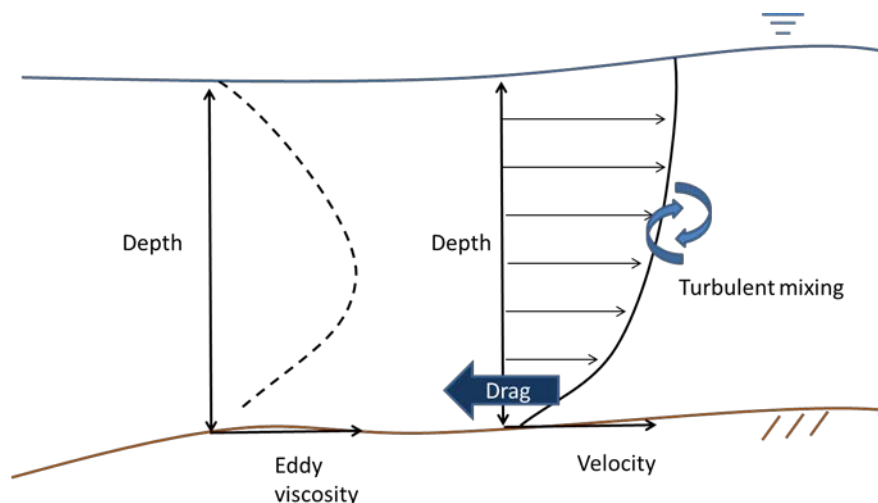
As with other semi-implicit layered models, SELFE can easily be applied in its single-layer 2-D form as well as in 3-D. Our preprocessing tools allow the domain to be cut at Martinez, above which the 2-D model can be used for model speedup; we are only beginning to explore this option.

**Figure 7-1 Bay-Delta SELFE Domain, Boundaries and Agricultural Source/Sink (DICU) Locations**



### 7.2.2 Roughness and Friction and Turbulence Closure

An important aspect of calibration is tuning the mechanism by which friction is imparted on flow. In SELFE, resistance is introduced into the water column through the combination of the bottom stress (drag) boundary condition felt just above the bed, and a vertical turbulent eddy viscosity that mixes the lower and higher velocity water (and salt) vertically. Figure 7-2 illustrates this process and also shows examples of how velocity and the eddy viscosity/diffusivity (mixing coefficient) might vary with depth.

**Figure 7-2 Typical Vertical Structure of Velocity (right) and Eddy Viscosity (left)**

In calibrating the model, there are three options in the stipulation of the drag coefficient:

- $C_d$  (drag) may be specified directly either as a constant or distributed over the mesh
- Roughness  $z_0$  may be specified, and  $C_d$  will be calculated as a function of depth from a standard formula describing the bottom boundary layer. This was our ultimate choice.
- In 2-D, Mannings coefficients can be given directly.

The turbulent eddy viscosity (and diffusivity for salt) are not stipulated directly, but rather emerge from the turbulence closure. We use the vertical component of Umlauf and Burchard's generic length-scale model, and two auxiliary differential equations which are integrated off-line of the other equations based on values from the previous time step. We found the results to be relatively insensitive to turbulence closure choice, except Mellor-Yamada closure, which tended to eliminate stratification. Work here is presented based on  $k - \epsilon$ .

### 7.2.3 Transport Equation

SELFE uses its transport module to track salt, temperature and sediment concentration, and water quality constituents. There are several algorithm choices in SELFE for constituent transport, and balancing these is critical for tuning model performance:

- First, order upwind finite volume method (FVM), which is faster but diffuses the vertical structure of salinity.
- Second, order total variation diminishing (TVD) upwind finite volume scheme, which is slower but preserves sharp gradients.
- Third, the Eulerian-Lagrangian Method (ELM) used for momentum advection, which combines (particle-like) backtracking along the velocity field with interpolation.

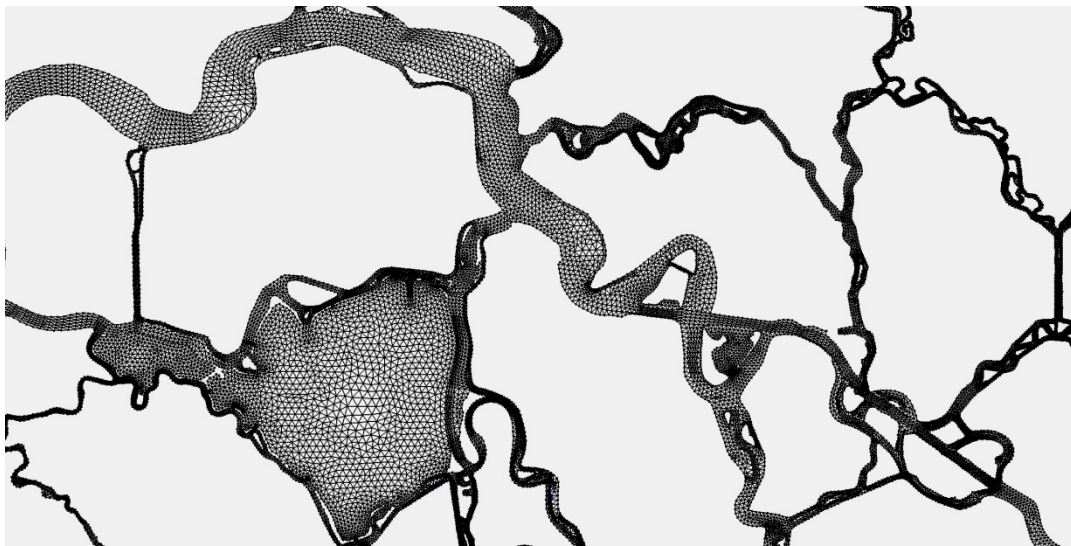
Because they are mass conservative, the two finite volume schemes are more commonly used than the ELM scheme. The two transport schemes can be mixed adaptively based on map and depth-based criteria. Specification of these criteria constitutes a calibration decision. Our use of the more expensive TVD method is limited to the region west of the confluence and to depths greater than 6m.

Horizontal diffusive mixing of constituent concentration is available, but not enabled. Velocity variation across the main flow field is directly resolved in most channels of importance, so modeling shear dispersion does not require a new term. Horizontal eddy diffusivity is very small compared to the other terms and enough is apparently introduced by the unavoidable horizontal numerical diffusion introduced in solving the equations.

#### 7.2.4 Horizontal Meshes

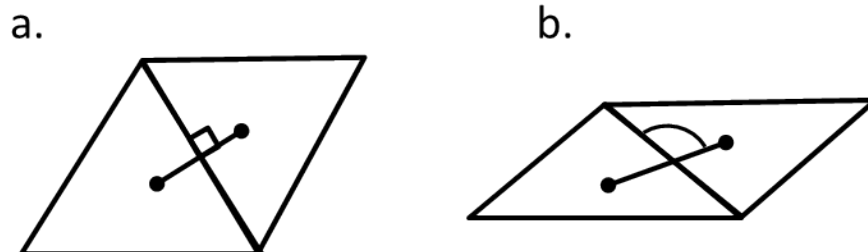
The horizontal mesh is referred to as *unstructured* because the connectivity of the triangles is general and unconstrained. The benefit of unstructured meshes is that they are easy to represent complex natural domains with a fair amount of accuracy (see Figure 7-3).

**Figure 7-3** Horizontal Mesh near Franks Tract



One additional distinguishing characteristic of the horizontal mesh used in SELFE compared to other semi-implicit models is that the mesh is not required to be *orthogonal* (Figure 7-4). In an orthogonal mesh, the edges of the mesh are perpendicular to the line between the "centers" (typically circumcenters) of the elements. For a triangular mesh, the orthogonality requirement leads to triangles that are nearly equilateral. While this shape is relatively efficient and accurate, generating such a mesh imposes tradeoffs with other desirable properties, such as conforming to the contours at the foot of a slope or thalweg of a channel.

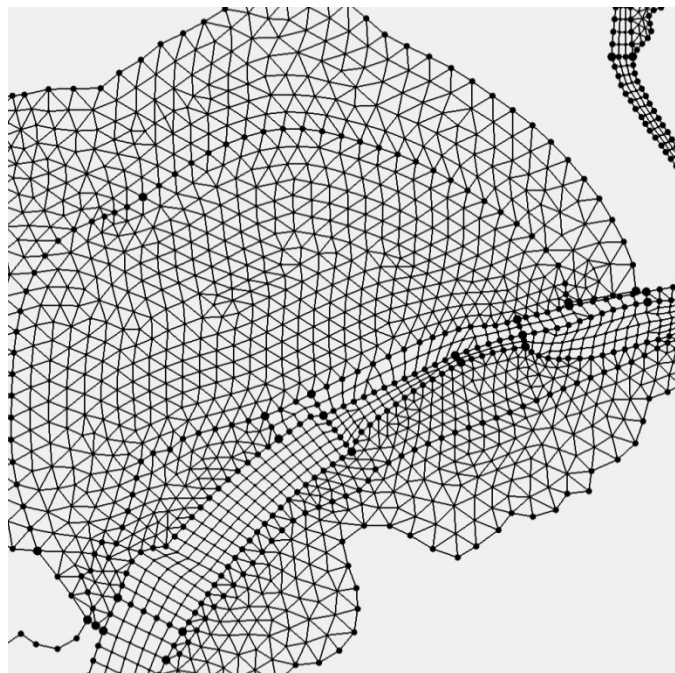
**Figure 7-4.** (a) Orthogonal Triangular Mesh. (b) Non-orthogonal Mesh with some Skew



One efficiency disadvantage in SELFE is that the mesh is limited to triangles. UnTRIM uses quadrilaterals. Newer versions of some other semi-implicit models (Deltares and SUNTANS) may allow more general element shapes, although, as far as we know, applications of these features are not ready. Some older models such as EFDC and the classic version of the Deltares 3-D model also have used quadrilaterals, but these are structured curvilinear quadrilaterals and are very restrictive when it comes to modeling natural systems.

The Bay-Delta mesh was constructed using the Aquaveo SMS model development software package (generic version), in which the user first specifies a skeleton mesh map comprised of discretized polygons each of which is then filled using automatic meshing algorithms. An advancing front algorithm ("paving") was used for large, well-resolved water bodies and some side embayments. Coons patches ("patching") were used in channelized areas, including internal channels in some bays and open water bodies. Figure 7-5 shows an example of the combination in preparation at San Pablo Bay, with Coons patches delineating the critical ship channel through Pinole Shoal Channel (the quadrilaterals will eventually be split into triangles) in an otherwise expansive embayment.

**Figure 7-5 Close-up of Mesh Preparation in San Pablo Bay with Coons Patches near Pinole Shoal**

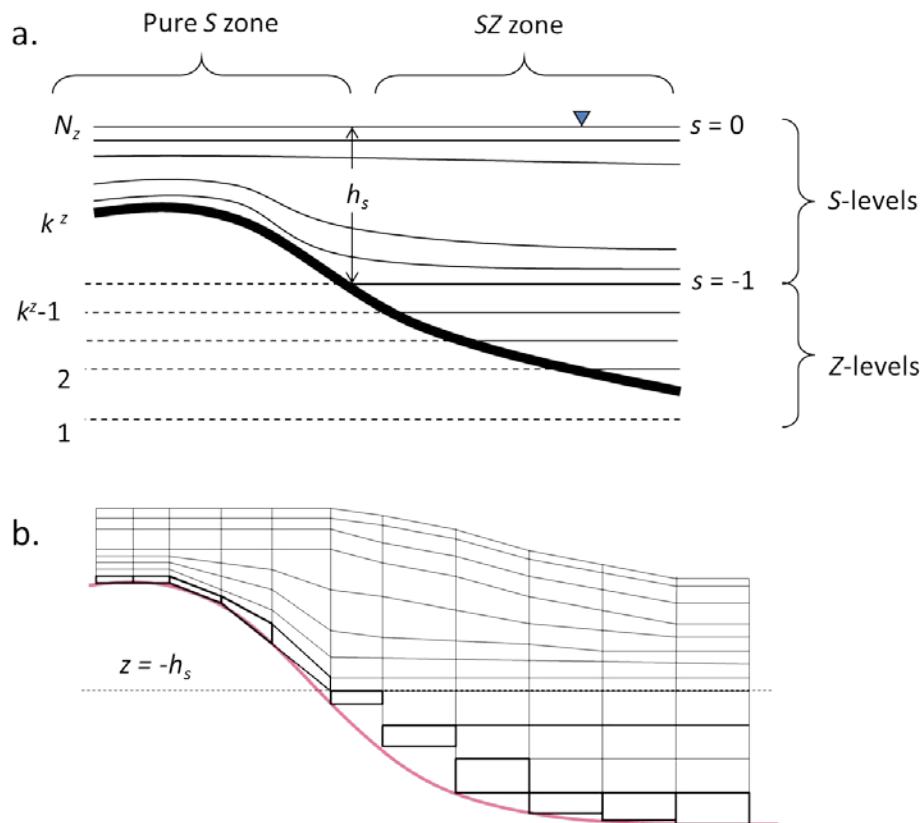


### 7.2.5 Vertical Mesh

SELFE has a flexible meshing system in the vertical direction, allowing a hybrid of Z layers below, and terrain-following S coordinates above, as shown in Figure 7-6. Z-layers are at fixed elevations, but the S-layers follow contours in the bed and allow the user to concentrate greater or less density in the lower or upper boundary layers. The original purpose of including the SZ hybrid was to avoid some of the pitfalls associated with topography-conforming meshes, particularly on very steep bathymetry in deep water. The Bay-Delta is generally shallow enough to avoid the Z layers entirely, so our mesh is defined by 23 vertical terrain-following S layers.

CMOP did extensive side-by-side testing of SELFE and ELCIRC, a Z-only model like UnTRIM and SUNTANS, and the terrain following mesh was one of the factors cited in the improved performance of SELFE for plume tracking. Although we are confident the pure-S approach is the best option available to us between S, Z, and SZ, we have also begun testing a vanishing quasi-sigma vertical coordinate system similar to that described by Dukhovskoy et al. (2009) in which layers disappear gradually in shallower water and therefore also have smaller gradients. Our implementation includes an enhancement to avoid the stairstepping noted by Dukhovskoy et al. (2009). This gridding system preserves the advantages of bathymetry conforming coordinates while reducing pressure errors, preserving stratification, and eliminating some practical issues associated with over-resolution in shallow water.

**Figure 7-6 (a) The Hybrid Coordinate System used in SELFE. S-Coordinates are used above the Threshold Depth, while Z (Stairstepping) Coordinates are used below.**  
**(b) Vertical Transect of an SZ Mesh**



### 7.2.6 Hydraulic Structures and Mass Sources

As part of the Bay-Delta SELFE project we added two capabilities to SELFE that were not part of the original code base. The first was the ability to model sub-grid hydraulic structures such as:

- Weirs, based on approximations in DSM2 and HEC-RAS,
- Culverts, based on simple orifice representations as in DSM2,
- Radial gates based on HEC-RAS,
- Direct transfers of water between subdomains.

Our implementation allows time series control of structures, as well as timed installation and full removal (in which case the location reverts to the usual hydrodynamic equations). In the near future we also plan to experiment with an energy-momentum approximation, for Clifton Court Forebay.

We also allowed a provision for mass sources and sinks, in order to accommodate Delta consumptive use (DICU). The mass addition is considered for purposes of continuity and transport but is not incorporated in the momentum equation.

## 7.3 Bay-Delta SELFE Application

### 7.3.1 Domain, Mesh, and Boundaries

The Bay-Delta domain encompasses a domain spanning from the Farallon Islands in the west, Knights Landing on the Sacramento River to the north, and Vernalis on the San Joaquin River to the south (Figure 7-1).

The ocean boundary of the Bay-SELFE model lies on a roughly 46 km radius arc from the Golden Gate, extending from Point Reyes to the Farallon Islands and south just past Half Moon Bay. The ocean boundary was chosen far enough offshore so that the dynamics inside the domain do not impact the boundary, including the discharge of sediment and fresh water plumes. For the simulations presented here, our boundary data is interpolated (inverse distance weighted) between Point Reyes and Monterey after which a fixed delay and scaling is applied everywhere along the boundary.

On the Sacramento River, the primary consideration was to model far enough upstream to avoid tidal reflection and facilitate a future extension to all of Yolo Bypass. To avoid complications and data shortages on the American and Feather rivers, flows on all three rivers are routed down the Sacramento. For flow data, we tidally filter U.S. Geological Survey (USGS) observations at Freeport and move the resulting time series upstream with a lead of 3 hours.

The other upstream boundaries and export sites are similar to those used by other community models including DSM2, data for which has been widely disseminated. The boundary data come from flow, pumping and conductance observations by USGS, DWR, and the U.S. Bureau of Reclamation (USBR). We made two additions for the Bay at Coyote Creek and Napa River.

The mesh comprises roughly 140,000 nodes and 238,000 triangles. Mesh resolution varies from approximately 1km in the ocean to 100-400m in the Bay and down to 20-60m in Delta channels, with the smallest element width less than 5m found near Middle River. Figure 7-7 shows a histogram of equivalent radii (i.e., radii of circles with equivalent area) of the elements, a measure of discretization length that tends to be on the small side – for anisotropic elements it tends to be smaller the width. The mesh sizing was chosen to:

- resolve bathymetric features and the deep sections of major channels, which is important for salinity intrusion,
- resolve lateral and vertical variations in velocity and shear dispersion,
- emphasize regions of policy importance or that have a greater effect on global accuracy,
- take good advantage of SELFE's ability to handle anisotropy and non-orthogonal elements.

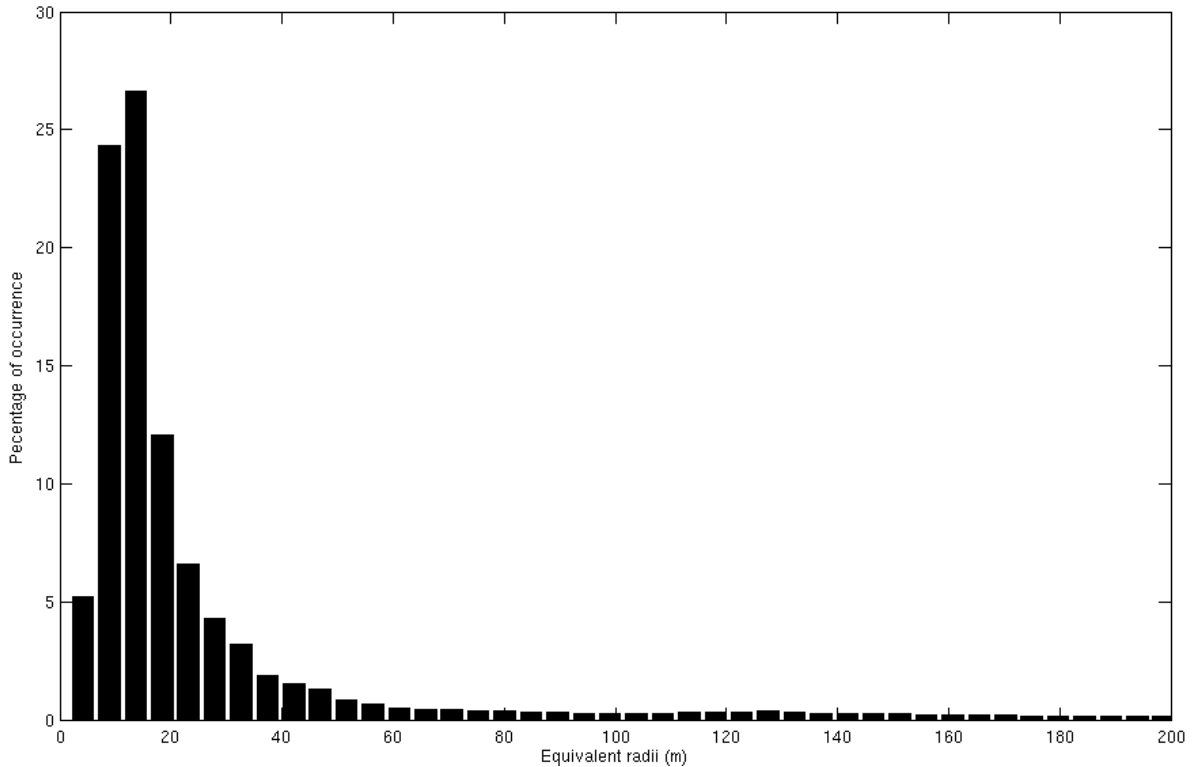
- realistically introduce wetting and drying while keeping always-wet main channels open to flow, and
- otherwise minimize computation time.

### 7.3.2 Bathymetry

SELFE requires bathymetry data at every node in the mesh. A lot of our early effort was spent collating and improving bathymetry. We described the generation of seamless topography models for multidimensional modeling in a previous annual report chapter. Several models are now utilizing this product and recently we have begun a more active exchange with the USGS resulting in better review and reconciliation of products.

Our bathymetry integrates elevation data from previous USGS maps, single and multibeam data collections into a set of mutually consistent 10m and 2m elevation DEMs. The data used in calibration is identical to the version 3 release of this bathymetry except that here we have incorporated recent improvements near the CVP intake and South Delta, and some additions in the north Sacramento River where we extended the bathymetry in response to boundary reflection.

**Figure 7-7 Histogram of Element Size, using Equivalent Radius (Radius of the Circle with Equal Area)**



Note: For anisotropic elements, equivalent radius is typically smaller than width.

Some re-processing of bathymetry was performed in order to better represent volumetric quantities and moments (volume, vertical face area) over the areas covered by mesh elements. In addition, in several marshy areas, such as Sherman Lake, we used contour-based smoothing methods to "untangle" very twisted subgrid topography so that the storage areas represented by intricate tertiary channels could be

captured better by the model. These additional geometry processing steps will be covered in some detail in the main calibration document.

The vertical datum of the model is NAVD88.

### 7.3.3 Barriers and Gates

All the major gate and hydraulic structures in the Bay-Delta system are included in our model, including the Delta Cross Channel, Montezuma Salinity Control Structure, south Delta temporary barriers, and the gate at Tom Paine Slough. Up to now, we have omitted some small structures in the Morrow and Roaring River complexes in Suisun Marsh where the channels are much smaller than our local model scale or where we do not yet feel we have mastered the connectivity. The fish barrier at the head of Old River was not installed for either of our two calibration years; it was, however, included for subsequent drought modeling in 2013-2014.

Gate timing and coefficients were taken mostly from institutional logs for the south Delta barriers, Suisun Marsh Gate (DWR), and Delta Cross Channel (USBR). The south Delta barriers were installed and removed using time series. A schedule of operations for 2009 and 2010 can be found respectively in Figures 7-8 and 7-9.

**Figure 7-8 Delta Hydraulic Structure Operations for 2009**

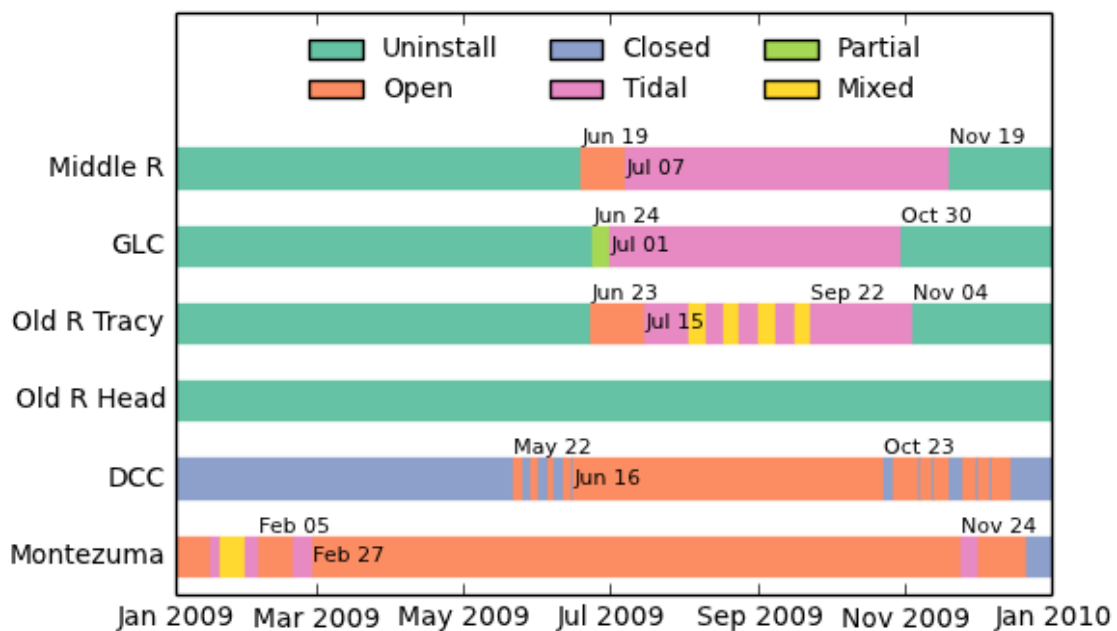
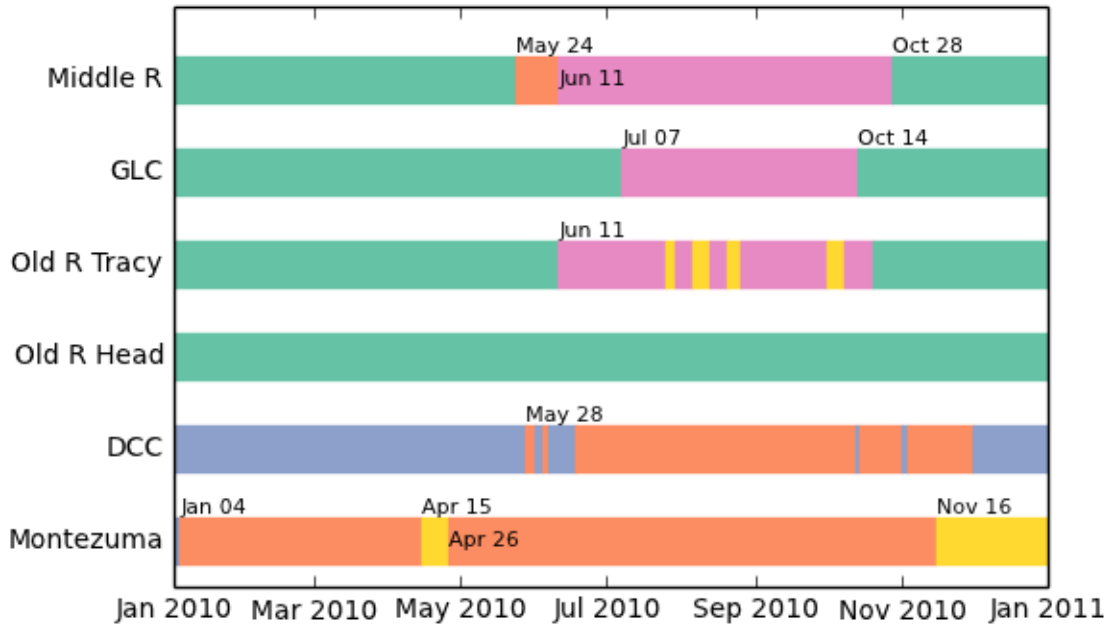


**Figure 7-9 Delta Hydraulic Structure Operations for 2010**



We modeled Clifton Court Forebay inflow using historical gate flows rather than as a radial gate. We were not confident that either the DSM2 rating or the Hills Equations used by Delta Field Division is sufficiently accurate to reproduce the water surface at Clifton Court or prevent gate flow errors from affecting the rest of the calibration. We have developed a rating for the gates based on several new data collections, and used it in the calibration to disaggregate daily gate flows in time as proposed by MacWilliams and Gross (2013). This solution works well for hindcast and calibration, though it has no analog in planning and small discrepancies between inflow and outflow can accumulate to unacceptable values over months. The new rating will be inserted inline in SELFE soon and used for long term historical and planning studies.

### 7.3.4 Atmospheric Inputs

The model accepts spatiotemporal atmospheric input representing surface wind, atmospheric pressure, and precipitation over the domain. The most significant of these is thought to be wind. There is no unified approach to modeling wind in the Bay-Delta region. Past work in the domain has either justified neglecting wind due to a short period of study or used atmospheric inputs from a small set of representative stations situated on the water.

The approach we adopted is to use climate or weather reanalysis products that combine a numerical model and data assimilation. Numerous reanalysis products are available for the region at both climate (coarser) and weather (finer) scales. For our calibration we used winds at 10m above ground from the NARR dataset from NOAA. This dataset is 32km in resolution, which is roughly the spacing of field stations used in and not fine enough to resolve the width of the Bay or local spatial patterns of wind at the Golden Gate, South Bay, San Pablo Bay, and Carquinez. Through our collaborators in the SESAME project, we have access to two much finer resolution wind fields from reanalysis products. The first is a 3km COAMPS model from the Central and Northern California Ocean Observing System (CenCOOS). The second is a 1km Weather Research and Forecasting (WRF) simulation from NASA unique to the

SESAME project. Preliminary results suggest high resolution data may not be required for global accuracy of salinity transport. This is a significant result because detailed wind data is not available in hypothetical situations, and will be particularly uncertain under climate change.

### 7.3.5 Initial Conditions

SELFE requires an initial condition for the entire model state, including velocity, water levels, and salinity. Initial conditions are quickly forgotten for water levels and velocities – and we use constants for these. The initial salinity field persists much longer, affecting the simulation for months.

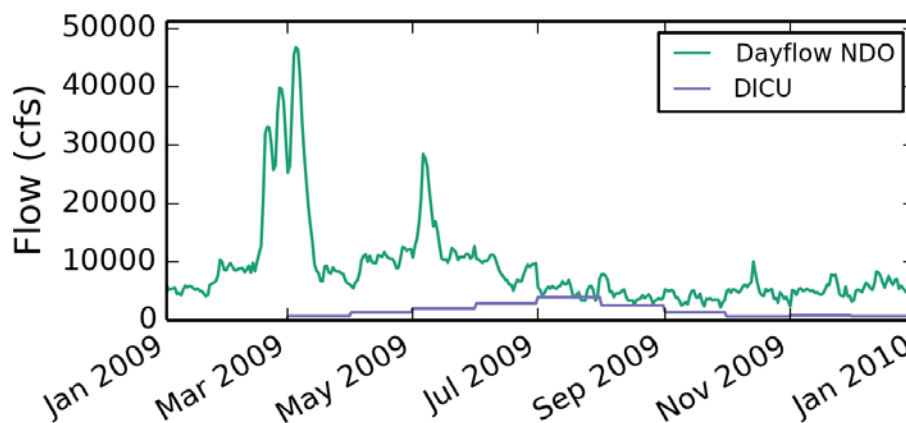
We use an estimated salinity condition from data to reduce spinup time for the model. Our salinity initial condition is generated regionally:

- Ocean: A scalar value of 33.5 psu at all depths, which is typical of the shelf region at modest depth.
- Bay and Suisun: From the south Bay to the confluence the model is initialized using vertical salinity profiles from USGS Polaris water quality cruises, interpolating linearly between stations and extrapolating radially from the path of the cruise.
- Delta: A scalar constant value of 0.1 psu (215 $\mu$ S/cm EC) is used throughout the Delta. This value is typical for the north Delta but too fresh for the south Delta.

During 2013-2014 drought modeling, salinity spinup in the south Delta took 3-4 months and limited our agility doing realtime runs with new grids. We recently started to minimize spinup time by briefly (3-5 days) assimilating data from the many observation stations in the Delta through a simple 2-D scheme called Newtonian Relaxation, or *nudging*. This technique more rapidly brings the model state very close to observed values anywhere that is within a few tidal excursions of a monitoring station.

### 7.3.6 Delta Agricultural Sources and Sinks (Consumptive Use)

The Delta islands are agricultural, and diversions and returns of water from the islands significantly impact flow and water quality in the channels. The magnitude of the water quality impact varies with the seasons, as the balance between diversions, drainage, and seepage changes. During summer months (including 2009), it is not uncommon for consumptive use to be equal in magnitude to total Delta outflow (see Figure 7-10, note the units are in cfs). This means that consumptive use is not only a major driver of local water quality, but also a near-dominant component of the flow balance preventing salinity intrusion from the ocean.

**Figure 7-10 Net Delta Outflow and Delta Island Consumptive Use Estimates for 2009**

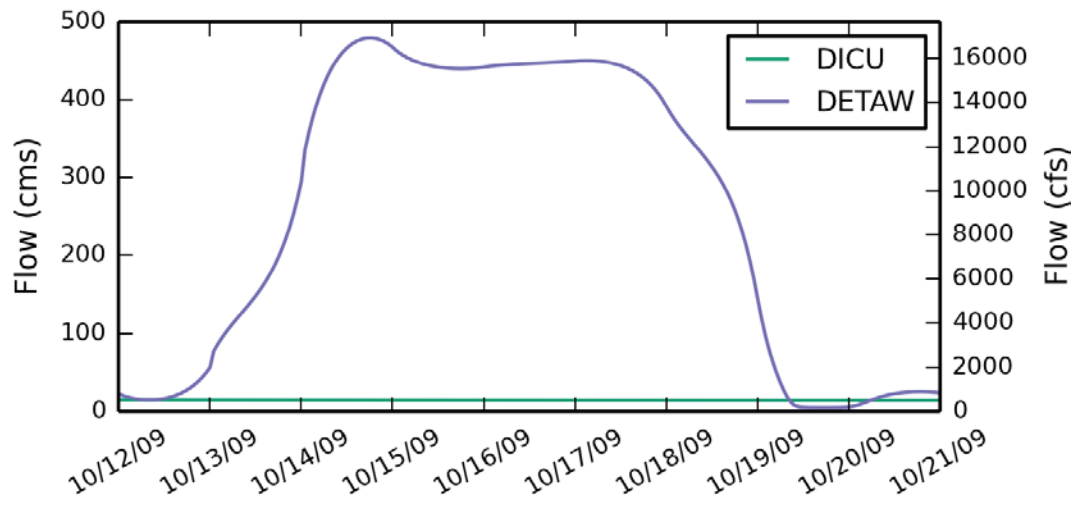
Historical flow and water quality data has not traditionally been available for the islands. In the absence of field data, we use estimates from the DWR Delta Island Consumptive Use model. The DICU model is centered on the islands (or regions), and performs a water balance that assumes land use and crop types and seeks to explain the resulting demand for water in terms of precipitation, soil moisture, seepage, and applied water. The inferred fluxes to and from the Delta channels are then assigned to discrete locations in a second step that is distinct from the water budget. Although the assignment of locations is based on survey locations, the original locations are aggregated and the final locations of the sources are influenced by the location of nodes in DSM2. The sites are shown in Figure 7-1.

In dry periods when salinity intrusion reaches the channelized Delta above the Sacramento-San Joaquin confluence, the uncertainty surrounding Delta outflow poses a confounding factor in any salinity calibration. Overall, we found the following two adjustments to DICU vastly improved agreement between model and data, including not only point observations but also vertical structure of salinity:

- For several days during big runoff events in 2009, we switched from DICU to DETAW, a beta-level daily consumptive use model being vetted to replace DICU. DICU, a monthly model, tends to undercalculate both the intensity and total volume of runoff from brief, intense storms (Figure 7-11). DETAW runoff data, Dayflow precipitation estimates and USGS outflow data all agree better.
- We scaled DICU so that outflow better matches seasonal fluctuations seen at the four USGS Net Delta Outflow gages (Sacramento River at Rio Vista, San Joaquin River at Jersey Point, Three Mile and Dutch sloughs).

Although these adjustments stem from observed data, they can still be problematic. Net flows at Jersey Point and Rio Vista are subject to substantial bias because they are extracted from tidal fluctuations orders of magnitude larger. The technique we used to correct outflow is limited to a short historical record and is brittle in some of those years including the winter 2013-2014. We are investigating newer methods that use the entire USGS and DWR flow observation network to better quantify Delta outflow.

**Figure 7-11 Estimates of Agricultural Drainage from DICU and DETAW Around the Period of the Storm**



### 7.3.7 Description

The period of the the calibration is March 12, 2009 through October, 2010. The year 2009 is categorized as dry and 2010 is categorized as below normal. The period through summer 2009 was used to match elevation and flow and the period through the first freshet in 2010 was used as the basis of matching salinity. Most of the results here come from the remainder of 2010, which was modeled twice, once following the calibration, and once after incorporating some changes from emergency drought modeling.

The hydrodynamics time step is 120 seconds for all the simulations, in keeping with the minimum time step to avoid numerical diffusion in the the Eulerian-Lagrangian component of the algorithm. The scalar transport part of the code is constrained by a different time step restriction, this one a maximum rather than a minimum, and as a result the transport regularly subcycles the main hydrodynamic time step using steps typically less than 30 seconds.

## 7.4 Calibration

The Bay calibration covers hydrodynamic variables (water surface, velocities, and cross-sectional flows) as well as salinity. The main items that we manipulated in the calibration were:

- horizontal mesh configuration, and density
- vertical mesh selection, configuration and density
- roughness coefficients
- the selection of turbulence closure
- the order of ELM interpolation at the foot of characteristics (i.e., after backtracking)
- extent over which higher order TVD transport was used.

In keeping with the practice in other 3-D Bay-Delta models, we did not adjust roughness spatially. We experimented with several relationships between roughness or drag and depth, but always applied the same formulas over the entire domain. We may relax this assumption later to acknowledge the influence of channelization, bed forms, and vegetation.

### 7.4.1 Computational Performance

The simulations reported in this chapter were performed on a Linux cluster with 180 cores at a ratio of simulated to computational time of 110:1, meaning that it takes roughly 3 days of computer time to simulate a year. We are currently working with a refined, less optimized grid that is somewhat slower at 85:1.

### 7.4.2 Skill Metrics for Scalar Station Data

For station data, we evaluate model performance based on both visual assessments of tidal and subtidal time series plots and quantitative fitness scores. Here, only a representative sample of stations is given for each variable of interest, illustrating typical results. We will make results for many more stations available online with the release of the calibration document.

The following statistics are reported where appropriate:

- **RMSE:** Root mean square error, not phase-corrected.
- **Lag:** An estimation of lag in minutes between the observed and modeled signal based on cross-correlation analysis, as described in RMA (2005). The phase lag estimated here is used to shift the series for calculation of the remainder of the metrics.
- **Bias<sub>φ</sub>:** The median bias of phase corrected error (modeled - observed)
- **NSE<sub>φ</sub>:** The Nash-Sutcliffe efficiency for the phase-corrected error:
  - $NSE\phi(f, r, x) = 1 - (MSE(f, x)/MSE(r, x))$
  - where  $MSE(f, x) = \frac{1}{n} \sum_{i=1}^n (f_i - x_i)^2$  is the mean squared error between a forecast or reference ( $f$ ), and an observation ( $x$ );  $r$  represents the station time-average.
- **R<sub>φ</sub>:** The correlation coefficient (the  $r$  in  $R^2$  for the fit of the observations on the phase-corrected model values.

Our main criteria for these metrics were robustness and consistency of approach with other Bay-Delta published calibrations. Following RMA (2005), we first estimate phase error and then correct for phase (by shifting the model output in time) when generating the remaining statistics except for RMSE.

### 7.4.3 Elevation

#### 7.4.3.1 Monitoring Stations

Continuous observations of elevation are available throughout the Bay-Delta, collected mainly by NOAA, DWR, and USGS. The instruments are precise, but there is considerable uncertainty concerning vertical datum – particularly in the Delta where subsidence is an issue.

Representative time series comparisons results and metrics are shown in Figures 7-12 through 7-14 on the Old River at Bacon Island, Sacramento River at Walnut Grove and I Street. Overall the fit is strong throughout the Bay and Delta. Subtidal fluctuations (changes slower than diurnal tides) are reproduced accurately over a variety of inflows, barometric fluctuation, and tidal energies. The tidal range at the

upstream sites on the Sacramento River and San Joaquin River illustrates a tendency towards underdampening, with tidal range and phase lead growing with propagation distance.

We have omitted time series results for most of the Bay, although we will include them in our more comprehensive reports. As the tidal results below hint, elevation results in the Bay have small errors.

### 7.4.3.2 Tidal Phase and Amplitude

A system-wide view of tidal propagation is given in 7-15 and 7-16, which map the amplitude and phase of the largest tidal constituent M2 (approximately 12.5 hour period) through the Bay-Delta system for both model and observations during April 2010. The amplitudes are in meters, phase is in minutes difference from arrival at the Golden Gate (not degrees).

The model reproduces tidal constituents very well through the Bay. Error is small and has no noticeable structure. Above the confluence, the model is underdamped, with model amplitude larger and phase earlier than observed. The amplitude error is modest mid-Delta, though it reaches 10% upstream on the Sacramento River and south Delta (but not along the Sacramento Ship Channel). Phase lead also begins above the confluence, with typical values of 15-30 minutes mid-Delta and higher values upstream. Despite some error, phase is gradual and regionally self-consistent – with care, the model does not create spurious potential differences between the main channels and side streams, a problem seen sometimes at Turner Cut with DSM2.

**Figure 7-12 Stage Results at Old River at Bacon Island**

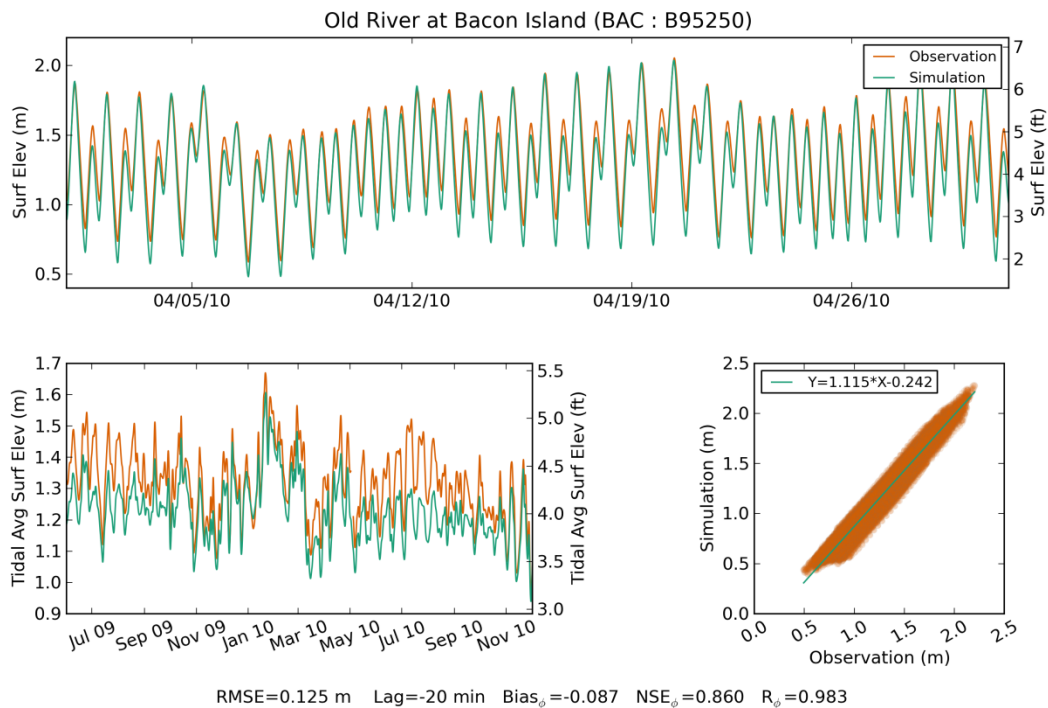


**Figure 7-13 Stage Results for Sacramento River at Walnut Grove**

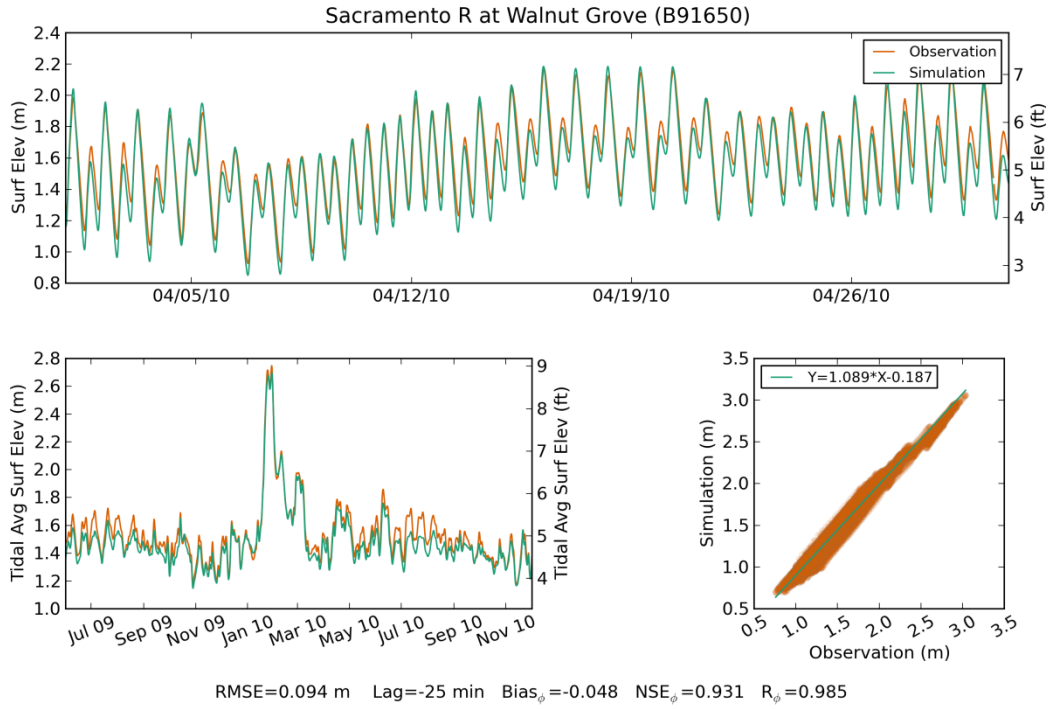


**Figure 7-14 Stage Results for Sacramento River at I Street**

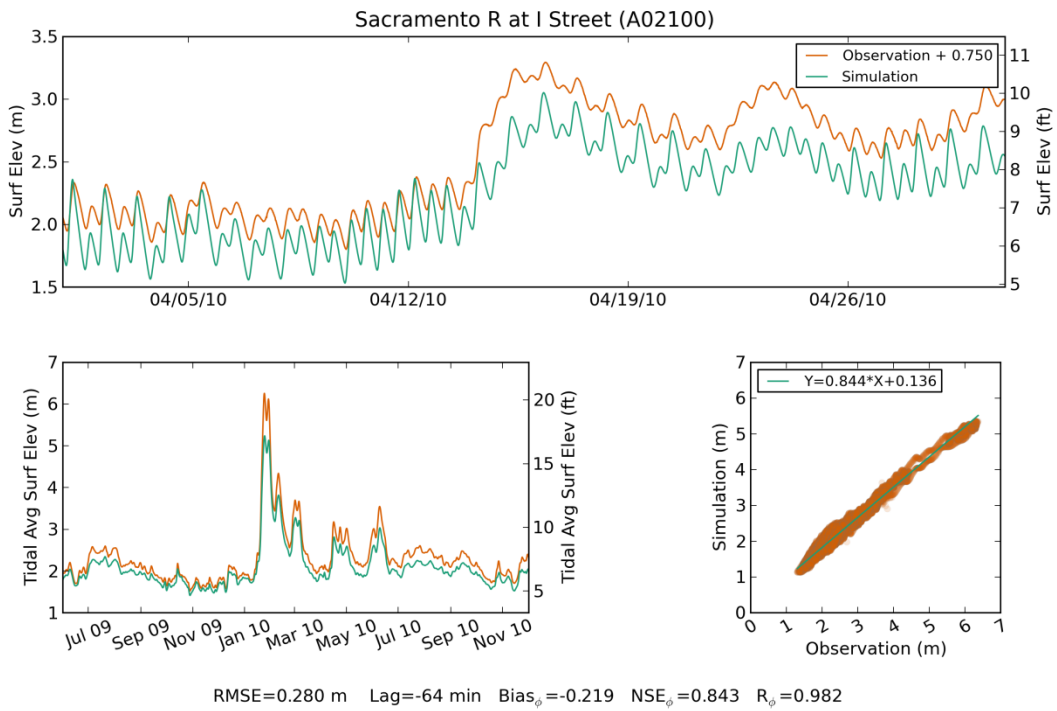


**Figure 7-15 Map of M2 Amplitude at Bay-Delta Stations, April 2010**

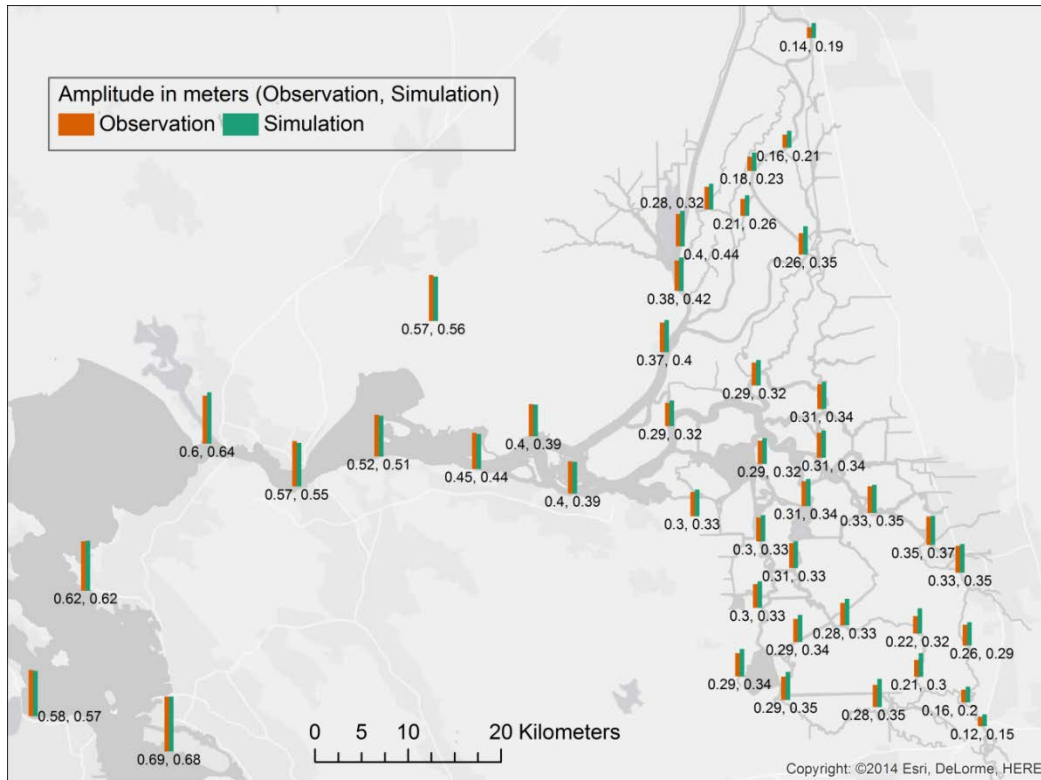
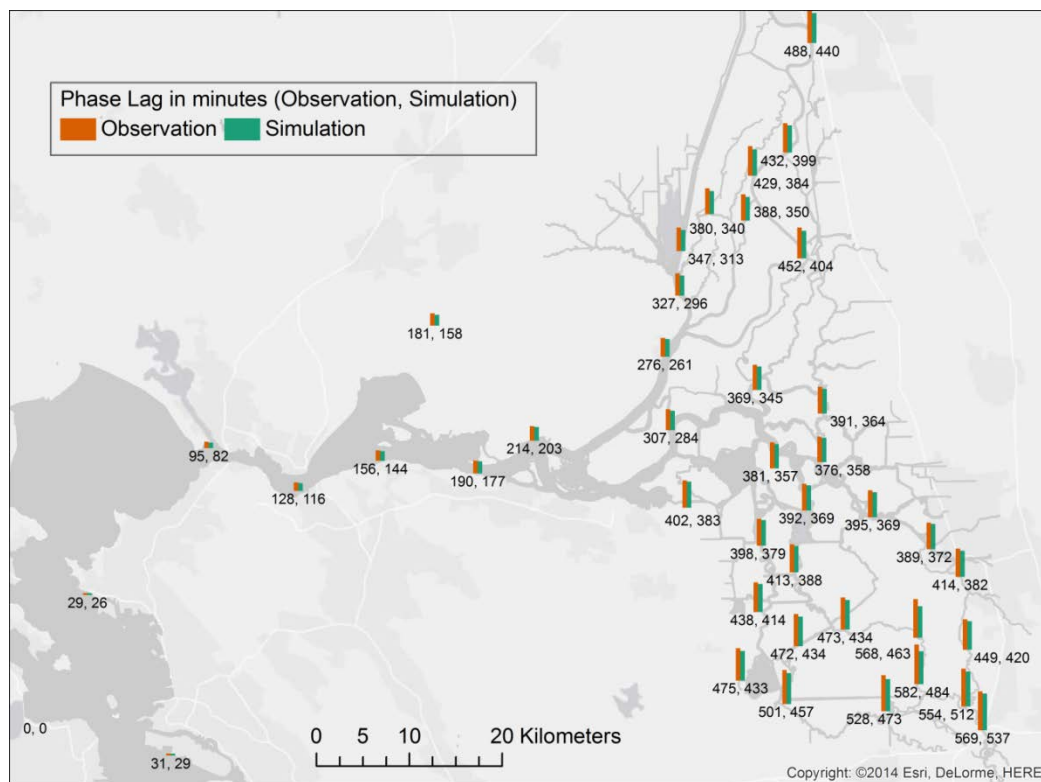


**Figure 7-16 Map of M2 Phase at Bay-Delta Stations, April 2010**



Note: The units are minutes of lag relative to San Francisco, not degrees.

### 7.4.4 Flow Results

Continuous flow monitoring stations are located throughout the Delta, operated primarily by the USGS and DWR. Flow observations are indirect, using surrogate *index velocity* measurements over part of the width of the river and relating them to total flow by a rating (linear or polynomial regression).

Flow results for two sample stations are shown in 7-17 and 7-18. Tidal range for most stations in the Delta is very good. A particularly good result is obtained at Three Mile Slough, a traditional site of difficulty because it is driven by potential differences between the Sacramento and San Joaquin river systems.

Some stations have slightly attenuated or amplified tidal ranges, as in the case of Old River at Quimby Island. The errors in flow tend to be local in character. As with elevation, flow is subject to some phase lead; in this case we believe the lead is caused by a combination of model error and the techniques used to rate flow instruments, a point we will elaborate upon in the near future.

**Figure 7-17 Flow Results at Three Mile Slough**

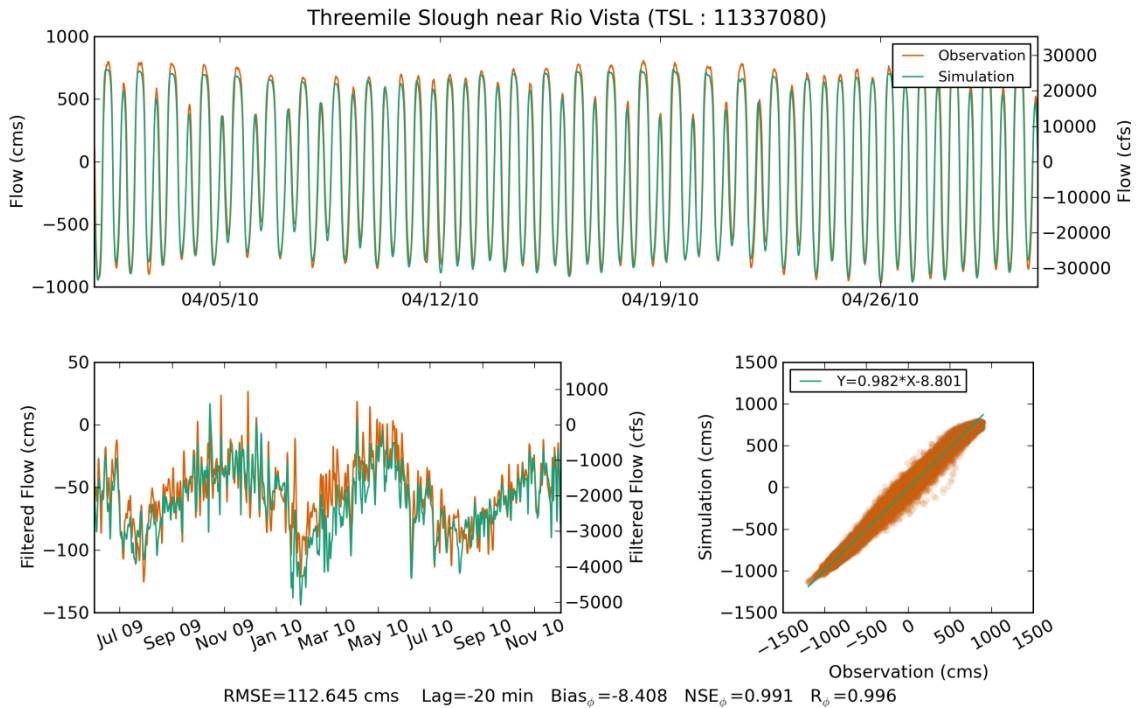
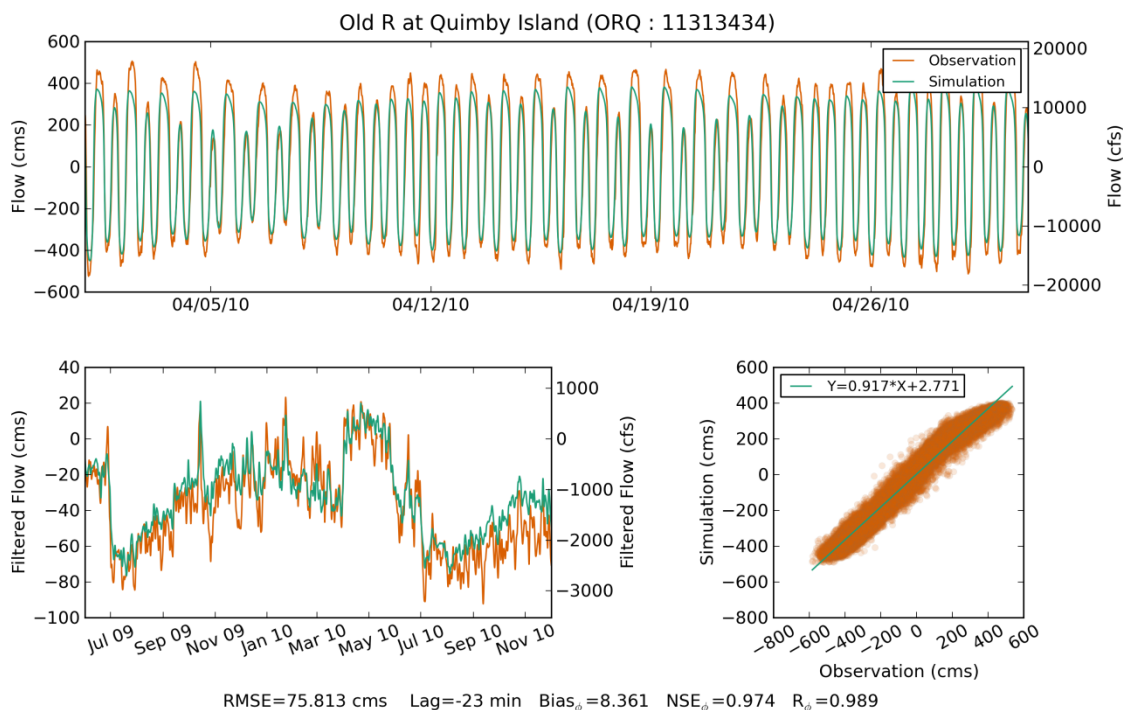


**Figure 7-18 Flow Results at Old River at Quimby Island**

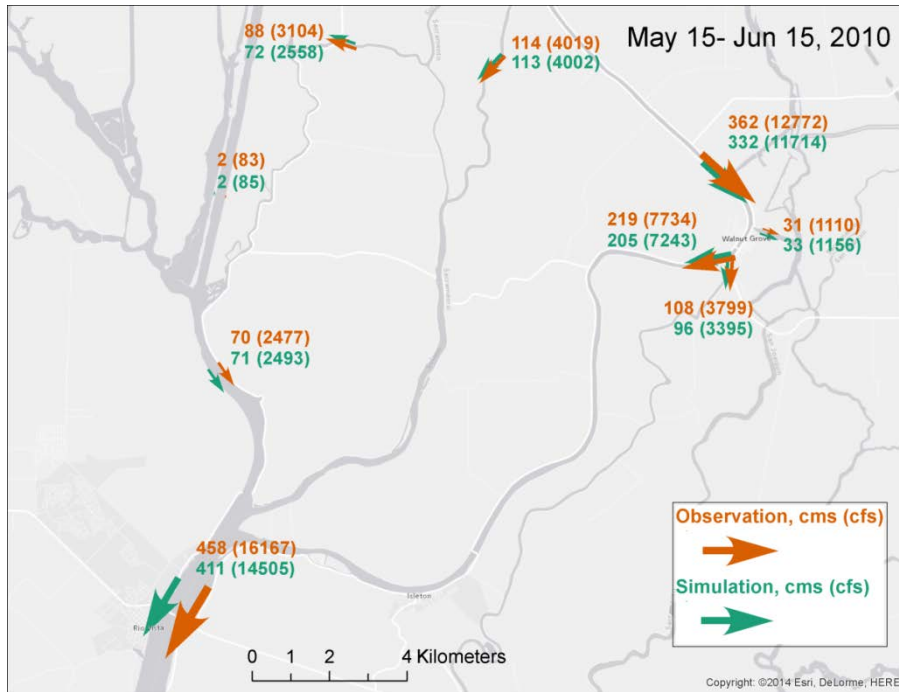


#### 7.4.4.1 Net Flow Maps

Net flow maps were used by RMA in to give a synoptic view of mean circulation in the Delta. *Net flow* here refers to residual flows after filtering to eliminate tidal frequencies or spring-neap variation. Residual flow is of some direct interest because it contributes to transport and residence time in the Delta – though the importance of the mean flow contribution to transport is often overestimated. Residual flow is also a diagnostic of how well we can model the details of tidal processes, since residual flows often manifest as small systematic asymmetries in a much larger tidal pattern. Observed data share some of the same challenges when averaged to produce a net flow. Calculations from observations from wide stations such as Rio Vista or Jersey Point carry a particularly strong caveat, and it is not uncommon for small control volumes constructed from a few neighboring stations to exhibit net flow discrepancies of hundreds or even thousands of cubic feet per second.

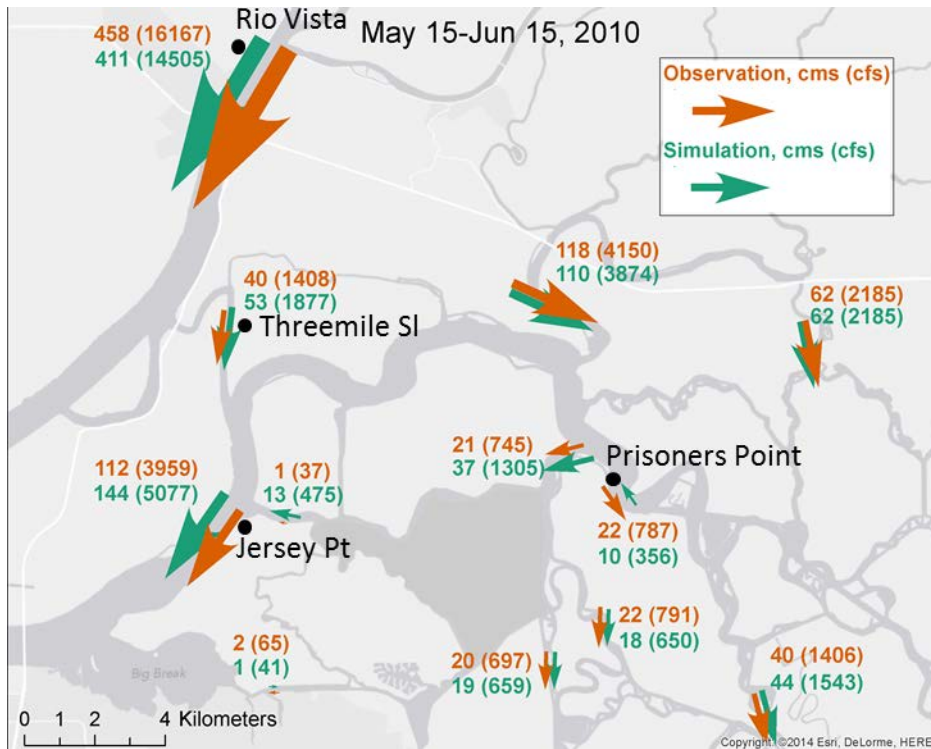
Figures 7-18 through 7-20 compare modeled and observed mean flow in the north, central, and south Delta for the month of May 15 through June 15, 2010. Barriers are installed late in the period. The general agreement of model with observations is commensurate with the quality of the data, best in the north and south Delta. Rio Vista and Jersey Point are 10-20% off. The null velocity point near Prisoners Point where net flow reverses in orientation seems to be off by a few kilometers but otherwise is correctly captured by the model.

**Figure 7-19 North Delta Monthly Residual Flow, May-June 2010**



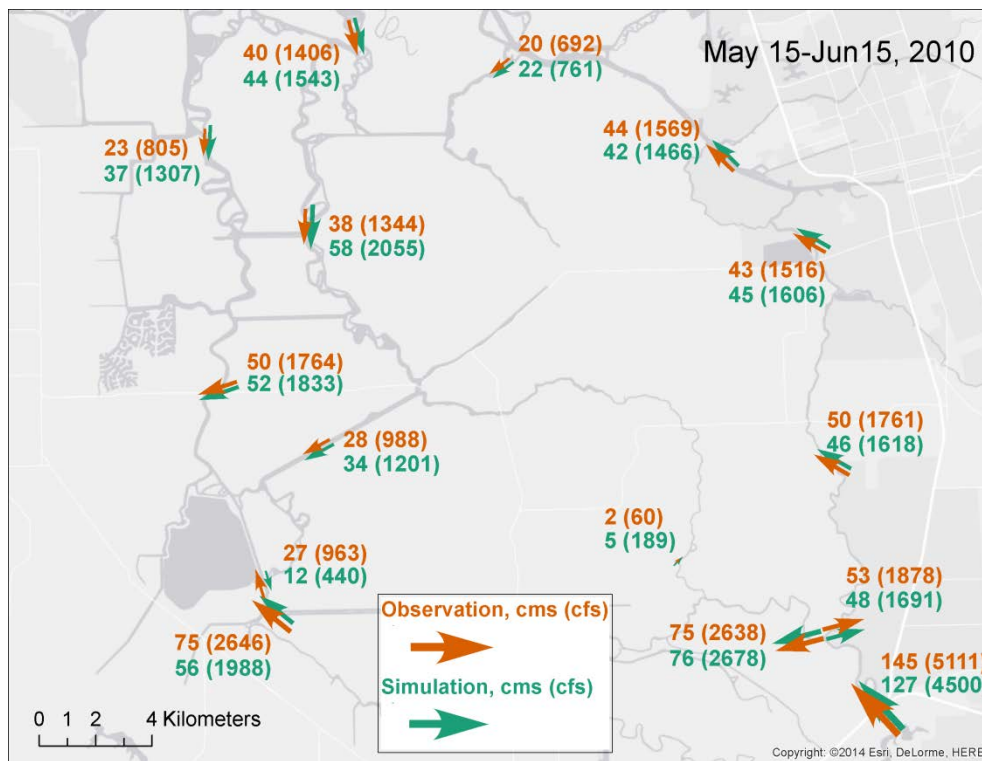
Note: Units are cms (cfs in parentheses)

**Figure 7-20 Central Delta Monthly Residual Flow, May-June 2010**



Note: Units are cms (cfs in parentheses)

**Figure 7-21 South Delta Monthly Residual Flow, May-June 2010**



Note: Units are cms (cfs in parentheses)

## 7.4.5 Salinity Results

### 7.4.5.1 Monitoring Stations

Salinity is mostly monitored in the form of electrical conductivity, (specific conductance) or EC, at more than 40 stations in channelized and open areas. Precision of the instruments is good, but observations of conductivity are noisy due to the high variability of salinity itself.

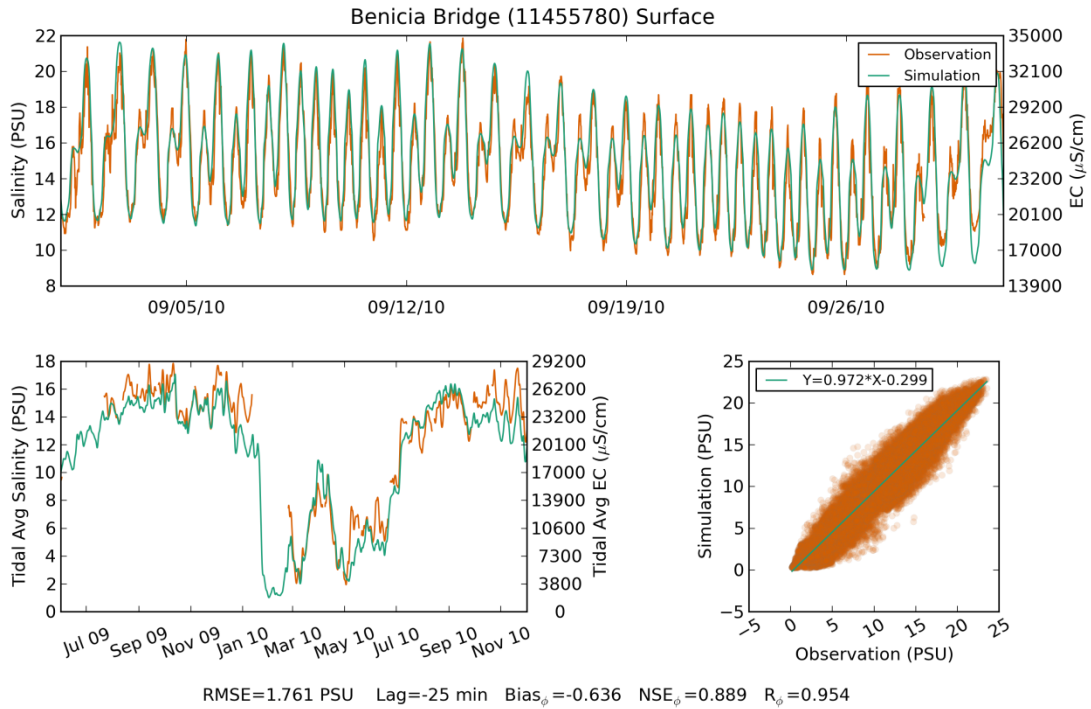
Figures 7-21 through 7-23 show salinity results at three sites in the Delta in late October, and for a lengthier period in 2009-2010 at subtidal scale. It is difficult to show all the regimes of interest in a summary document. Our results here focus on salinity at Benicia, Rock Slough, and Clifton Court.

Benicia salinity is similar to that at Martinez, a site of interest to Delta modelers. The advantage of the Benicia location is that it is mid-stream and less affected by local bathymetry. Surface salinity plots at Benicia indicate the model reproduces salinity with a modest bias and RMSE error that is distributed fairly evenly between trend, tidal frequencies, and noise.

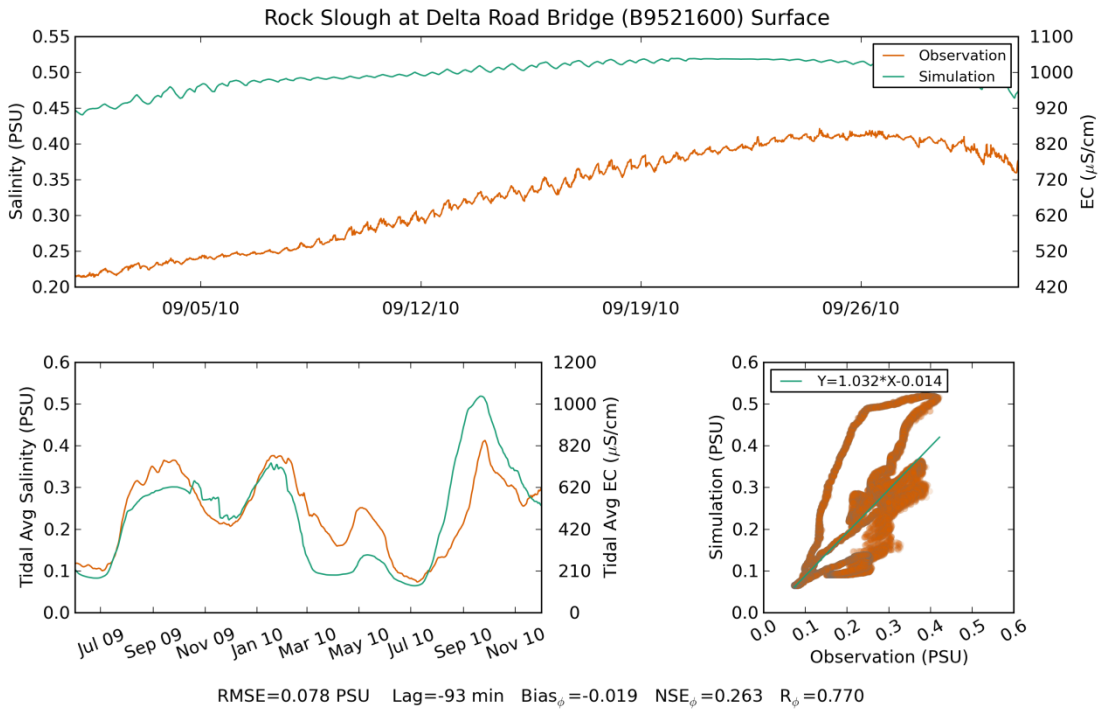
Rock Slough and Clifton Court follow seasonal trends well and have errors comparable to other models although the Nash skill metrics for Clifton Court are low. Stations between Antioch and Clifton Court were afflicted by an episode of over-intrusion of ocean salinity in late summer 2010, the recovery from which is evident in the beginning of the tidal-scale plots. This over-intrusion episode was timed almost exactly at the point when DICU becomes a dominant contributor to outflow error. The sensitivity – and

potential over-sensitivity – of the model to sustained periods of low outflows is still an area of active investigation for us.

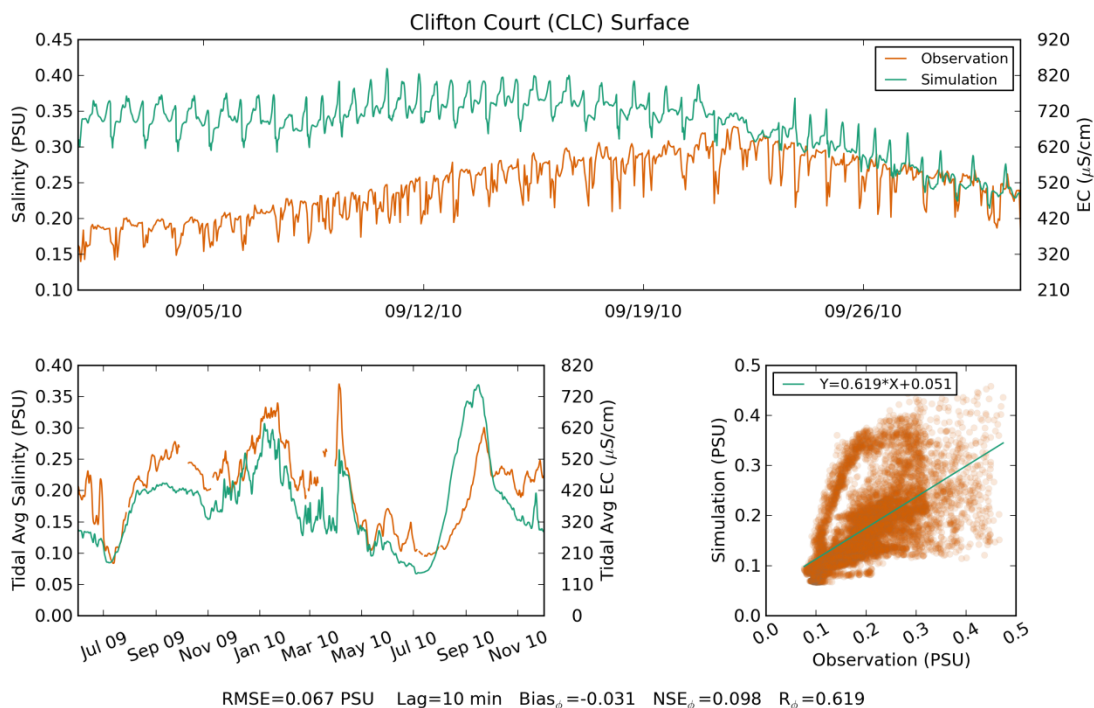
**Figure 7-22 Salinity Results at Benicia (Surface)**



**Figure 7-23 Salinity Result at Rock Slough**



**Figure 7-24 Salinity Result at Clifton Court**



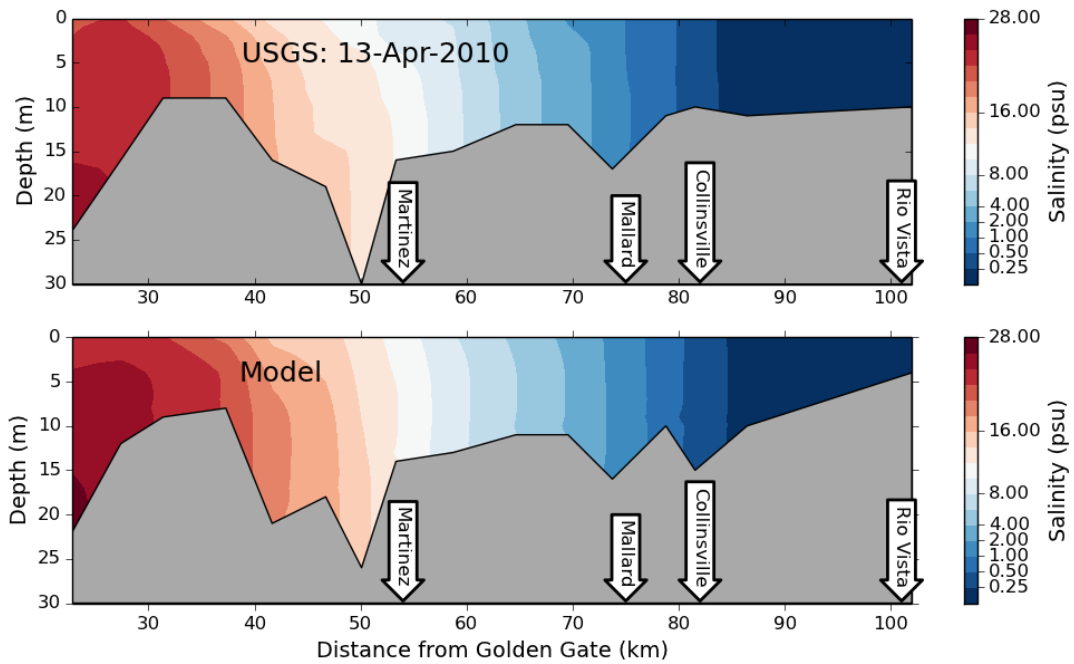
The USGS Polaris cruise (<http://sfbay.wr.usgs.gov/access/wqdata>) is a longitudinal profile of vertical conductivity-temperature-depth (CTD) casts from the south Bay to Rio Vista. Full or partial cruises are made once per month and have been used to validate the vertical or horizontal distribution of salinity in the Bay part of the domain, particularly for UnTRIM. The sites visited by the Polaris are shown in Figure 7-24. The northern leg of the cruise takes 6 hours; along its course it samples water at both extremes of a tidal excursion and therefore at minimum (typically zero) and maximum values of strain-induced stratification. So in terms of vertical structure the cruise is not a snapshot. There are also differences between observed and modeled bathymetry in the plots and these arise from slight deviations from scheduled locations along the cruise.

Figure 7-25 compares model and observed data between the Golden Gate and Rio Vista for a cruise in April 2010. Agreement is good for most isohalines of interest. Such stratification as exists in the observations (mostly in San Pablo Bay) is well reproduced down to 0.5 psu. At very low salinities (e.g. 0.25 psu or roughly 500 µmhos/cm EC), the sensitivity to outflow is higher.

**Figure 7-25 USGS Polaris Cruise Sample Locations**



**Figure 7-26 USGS Observations and SELFE Model Output for the Northern Leg of an April 13, 2010 Cruise**



Note: Travel time for this leg is approximately 6 hours

#### 7.4.5.2 Stratification Plots

The Polaris cruises give some indication of vertical structure, particularly persistent stratification in the lower estuary. Unfortunately, the cruises seldom coincide with major stratification events, particularly in the Carquinez Strait region. This can pose a challenge for calibration and validation. Even the stratification events categorized as large based on San Pablo Bay are only 2-3 psu on both sides of the strait, whereas stratification of 6 psu is a common peak in average neap tides and values of 10-12 psu are seen several times annually.

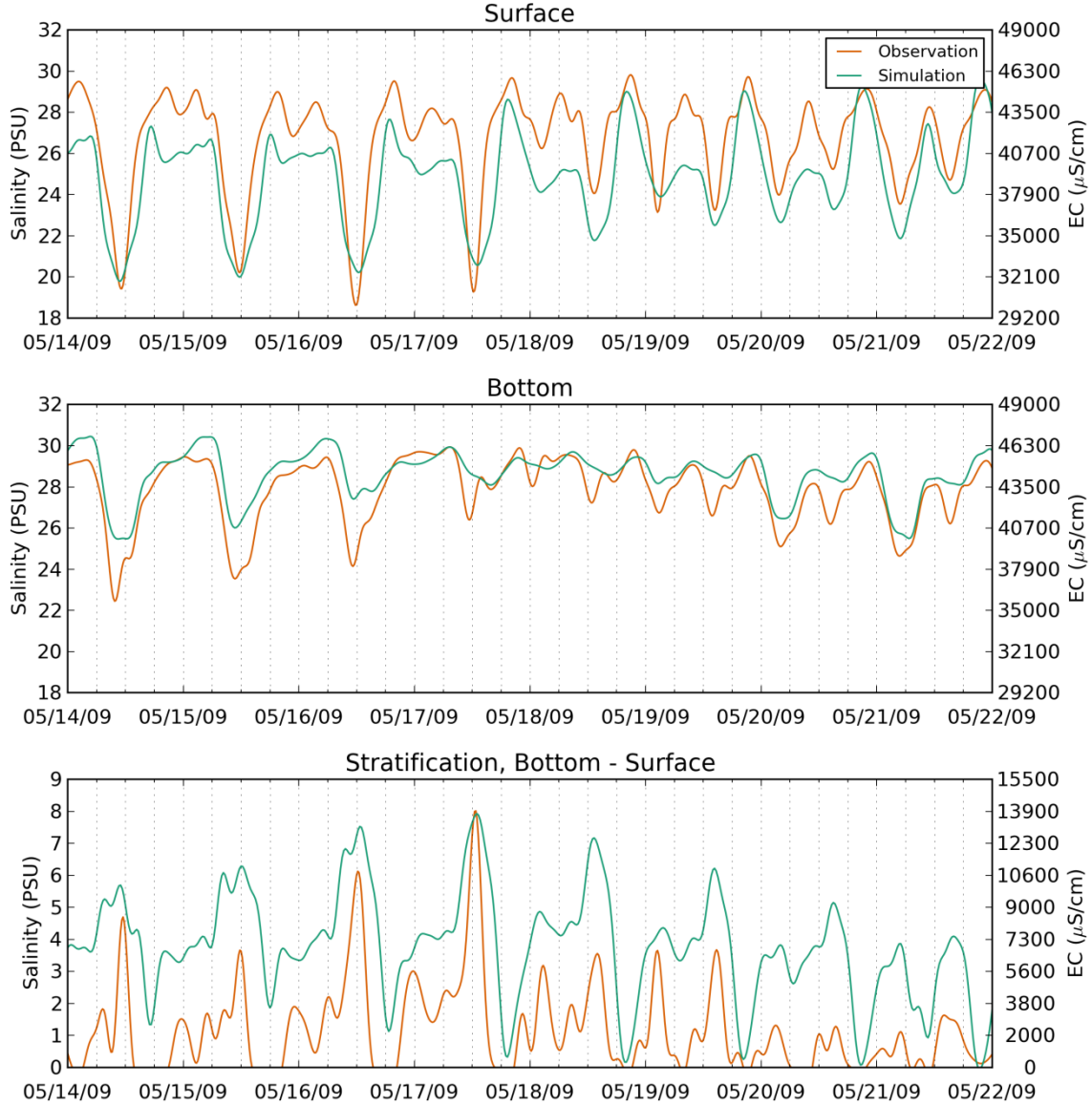
Another approach, fraught with different difficulties, is to look directly at time series of top and bottom salinity at mid-stream stations. SUNTANS stratification was compared to data from the upper and lower sensors on the Richmond and Benicia bridges and the authors were able to reproduce events of up to 8 psu on a short simulation with some success, although the accuracy varied regionally. This variation is to be expected as model forcing and horizontal transport problems cascade into stratification error.

Figure 7-26 through 7-28 shows results at Richmond and Benicia bridges for a 3-4 day stratification episode at neap tide in May 2009. Data have been low-passed with a cosine-Lanczos filter with cutoff frequency of 1/3 hour. The results are early in our calibration period, not from 2010, but seem to be somewhat typical. Provided the plume is located correctly horizontally, the model does a good job picking up very large stratification at Richmond. In contrast, the model under-predicts the largest events at Benicia, although it correctly identifies the transitions between periodic stratification and multi-day episodes.

We are still honing the model to reproduce the pycnocline better at Benicia. The error seems to be confounded by the placement of the sensor – something that we have not yet clarified. Figure 7-26 shows the high sensitivity of model stratification to the depth at which the bottom salinity is sampled – stratification nearly doubles between our original placement (-13.7m NAVD) and locations several meters deeper.

**Figure 7-27 Observed Top and Bottom Salinity and Stratification at Richmond Bridge**

Richmond-San Rafael Bridge (375607122264701)



**Figure 7-28 Observed Top and Bottom Salinity and Stratification at Benicia Bridge**

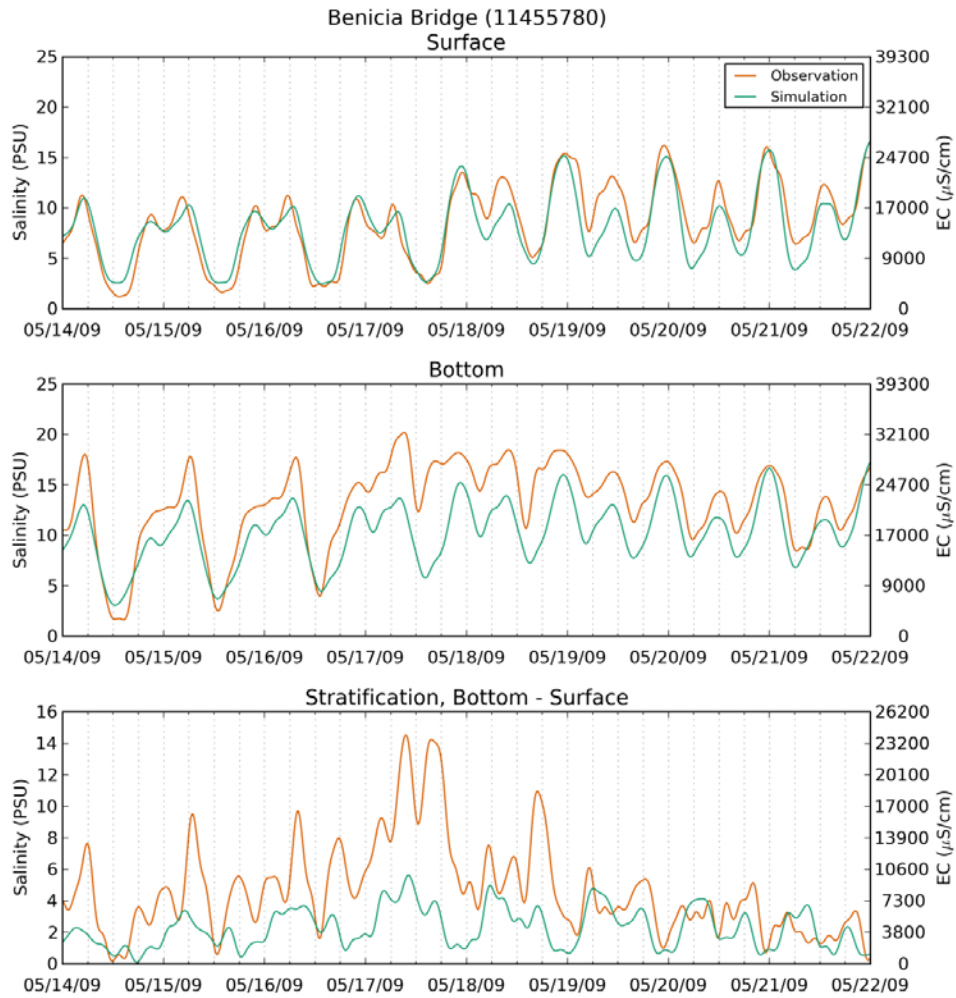
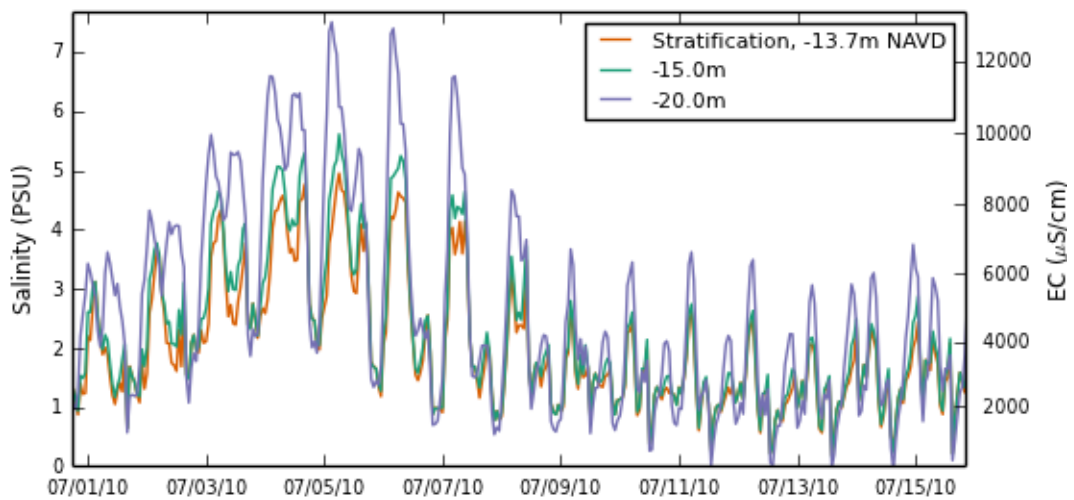


**Figure 7-29 Sensitivity of Salinity Stratification to the Placement of the "Bottom" Sensor**



Note: The timing of this plot does not coincide with that of Figure 7-27.

## 7.5 Conclusions

Our results suggest the suitability of the Bay-Delta SELFE model for use in multi-scale, system-wide estuary modeling, and as a far field background model for more focal studies. The model reproduces free surface elevation, flow, and salinity throughout the system with few standout issues. The model reproduces residual circulation in the Delta well. It reproduces vertical structure of salinity in the lower estuary where stratification plays its greatest role in transport; however, it underestimates the largest events at Benicia. Many of our target applications involving salinity, such as climate change analysis and flooded island studies, can be undertaken with the current model with little modification.

A calibration document is expected to be released soon after the publication of this chapter. It will contain additional detail about the formulation of the model and links to more comprehensive time series plots. We will also describe some qualitative features we have used to cross-check the model, including particle tracking evaluation of tidal excursion at Franks Tract and comparison with high frequency HF radar pictures of mean surface currents.

Additional validation materials will be developed in the next year covering the subjects of cross-sectional structure of salinity and velocity; horizontal variation of tidal phase and cross-stream velocity in tidal channels. Upcoming projects near Liberty Island and Yolo Bypass will also give us an opportunity to study the response of the model near breached levees and in overland flow. A temperature calibration is expected in the next year.

Some areas for further improvement are suggested by our results. These include a better or more conclusive understanding of equilibrium response to very low outflow, investigation of the onset of underdampening at the confluence, and improvement of bottom salinity at Benicia during large episodes of gravitational circulation.

Much of our focus in the coming few years will center on usability – things like the model interface, speed, and diversity of platforms. We have managed to double the speed for the Bay-Delta domain since beginning the project and hope to repeat this increase in performance. We have begun compiling the code on Windows with an aim to producing a 2-D model of the Delta.

## 7.6 References

- [1] G. L. Bodhaine. *Measurement of peak discharge at culverts by indirect methods*, Chapter A3. USGS, 1968.
- [2] P. R. Carlson and D. S. McCulloch. Aerial observations of suspended sediment plumes in San Francisco Bay and the adjacent Pacific Ocean. *U.S. Geological Survey, Journal of Research*, 2:519 – 526, 1974.
- [3] V. Casulli and P. Zanolli. High resolution methods for multidimensional advection-diffusion problems in free-surface hydrodynamics. *Ocean Modelling*, 10(77):137 – 151, 2005.

- [4] V. Casulli. A semi-implicit finite difference method for non-hydrostatic, free-surface flows. *Int. J. Numer. Methods Fluids*, 30:425 – 440, 1999.
- [5] V. P. Chua and O. B. Fringer. Sensitivity analysis of three-dimensional salinity simulations in north san francisco bay using the unstructured-grid suntans model. *Ocean Modelling*, 39(3 - 4):332 – 350, 2011.
- [6] A. Clemmens, T. Strelkoff, and J. Replogle. Calibration of submerged radial gates. *J. Hydraul. Eng.*, 129(9):680 – 687, 2003.
- [7] S. Danilov. Ocean modeling on unstructured meshes. *Ocean Modelling*, 69:195 – 210, 2013.
- [8] E. P. Dever and S. J. Lentz. Heat and salt balances over the northern California shelf in winter and spring. *Journal of Geophysical Research: Oceans*, 99(C8):16001 – 16017, 1994.
- [9] D.S. Dukhovskoy, S. L. Morey, P. J. Martin, J. J. O. Brien, and C. Cooper. Application of a vanishing, quasi-sigma, vertical coordinate for simulation of high-speed, deep currents over the Sigsbee Escarpment in the Gulf of Mexico. *Ocean Modelling*, 28(4):250 – 265, 2009.
- [10] R. L. Haney. On the Pressure Gradient Force over Steep Topography in Sigma Coordinate Ocean Models. *J. Phys. Oceanogr.*, 21:610 – 619, 1991.
- [11] E. Hills. New flow equations for clifton court gates. Technical report, California Department of Water Resources, State Water Project Division of Operations and Maintenance, 1988.
- [12] R. Holleman, O. Fringer, and M. Stacey. Numerical diffusion for flow aligned unstructured grids with application to estuarine modeling. *Int. J. Numer. Methods Fluids*, 72:1117–1145, 2013.
- [13] M. P. Hurst and K. W. Bruland. The effects of the San Francisco Bay plume on trace metal and nutrient distributions in the Gulf of the Farallones. *Geochim. Cosmochim. Acta*, 72:395 – 411, 2008.
- [14] M. Jung. Revision of Representative Delta Island Return Flow Quality for DSM2 and DICU Model Runs. Consultant Report to DWR MWQI-CR#3, 2000.
- [15] M. L. MacWilliams and E. S. Gross. Hydrodynamic Simulation of Circulation and Residence Time in Clifton Court Forebay. *San Francisco Estuary and Watershed Science*, 11(2), 2013.
- [16] M. L. MacWilliams, F. G. Salcedo, and E. S. Gross. San Francisco Bay-Delta UnTRIM Model Calibration Report, POD 3-D Particle Tracking Modeling Study. Technical report, Prepared for California Department of Water Resources, 2008.
- [17] M. L. MacWilliams, F. G. Salcedo, and E. S. Gross. San Francisco Bay-Delta UnTRIM Model Calibration Report, Sacramento and Stockton Deep Water Ship Channel 3-D Hydrodynamic and Salinity Modeling Study. Technical report, Prepared for US. Army Corps of Engineers, San Francisco District, 2009.

- [18] H.F. Matthias. *Measurement of Peak Discharge at With Contractions by Indirect Means*, Chap A4. Number 03-A4 in *Techniques of Water-Resource Investigation*. USGS, 1967.
- [19] N. Mahadevan. *Estimation of Delta Island Diversions and Return Flows*. California Department of Water Resources, Division of Planning and Local Assistance. Sacramento, CA, 1995.
- [20] M. Noble. Current patterns over the continental shelf and slope. Technical report, U.S. Geological Survey, 2001.
- [21] J. Oliger and A. Sundström. Theoretical and practical aspects of some initial boundary value problems in fluid dynamics. *SIAM J. Appl. Math.*, 35(3):419–446, 1978.
- [22] P.-O. Persson and G. Strang. A simple mesh generator in matlab. *SIAM Review*, 46:329–345, 2004.
- [23] P.-O. Persson. *Mesh Generation for Implicit Geometries*. PhD thesis, MIT, 2005.
- [24] D. K. Ralston and M. T. Stacey. Shear and turbulence production across subtidal channels. *Journal of Marine Research*, 64:147 – 171, 2006.
- [25] Saul Edward Rantz. Measurement and computation of streamflow: Volume 2, computation of discharge. TechReport 2175, USGS, 1982.
- [26] RMA. Flooded islands pre-feasibility study rma delta model calibration report. Technical report, Prepared For: California Department of Water Resources For Submittal To California Bay-Delta Authority, 2005.
- [27] C. A. Ruhl, D. H. Schoellhamer, R. P. Stumpf, and C. L. Lindsay. Combined Use of Remote Sensing and Continuous Monitoring to Analyse the Variability of Suspended-Sediment Concentrations in San Francisco Bay, California. *Estuarine, Coastal and Shelf Science*, 53:801 – 812, 2001.
- [28] A. F. Shchepetkin and J. C. McWilliams. The regional oceanic modeling system (ROMS): A split-explicit, free-surface, topography-following-coordinate oceanic model. *Ocean Modelling*, 9:347 – 404, 2005.
- [29] J. R. Siddorn. An analytical stretching function that combines the best attributes of geopotential and terrain-following vertical coordinates. *Ocean Modelling*, 66:1 – 13, 2013.
- [30] Y. Song and D. Haidvogel. A Semi-implicit Ocean Circulation Model Using a Generalized Topography-Following Coordinate System. *J. Comput. Phys.*, 115(1):228 – 244, 1994.
- [31] C. A. Stow, J. Jolliff, D. J. McGillicuddy Jr, S. C. Doney, J. I. Allen, M. A. M. Friedrichs, K. A. Rose, and P. Wallhead. Skill Assessment for Coupled Biological/Physical Models of Marine Systems. *Journal of Marine Systems*, 76:4–15, 2009.

- [32] B. Suits. Calibrating dsm2-quality dispersion factors to practical salinity. In *Methodology for Flow and Salinity Estimates in the Sacramento-San Joaquin Delta and Suisun Marsh 23rd Annual Progress Report*, 2002.
- [33] L. Umlauf and H. Burchard. A generic length-scale equation for geophysical turbulence models. *Journal of Marine Research*, 61:235 – 265, 2003.
- [34] J. R. Villemonte. Submerged-weir discharge studies. *Engineering News Record*, pages 54–57, 1947.
- [35] T. L. Wahl. Refined Energy Correction for Calibration of Submerged Radial Gates. *Journal of Hydraulic Engineering*, 131(6):457–466, 2005.
- [36] R. Wang and E. Ateljevich. A Continuous Surface Elevation Map for Modeling. Technical report, California Department of Water Resources, Bay-Delta Office, Delta Modeling Section, 2012.
- [37] C. J. Willmott, S. G. Ackleson, R. E. Davis, J. J. Feddema, K. M. Klink, D. R. Legates, J. O’Donnell, and C. M. Rowe. Statistics for the evaluation and comparison of models. *Journal of Geophysical Research: Oceans*, 90(C5):8995 – 9005, 1985.
- [38] C. J. Willmott, S. M. Robeson, and K. Matsuura. A refined index of model performance. *International Journal of Climatology*, 32(13):2088 – 2094, 2012.
- [39] C. J. Willmott. Some Comments on the Evaluation of Model Performance. *Bull. Amer. Meteor. Soc.*, 63:1309 – 1313, 1982.
- [40] Y. Zhang, A. M. Baptista, and E. P. Myers. A cross-scale model for 3D baroclinic circulation in estuary-plume-shelf systems: I. Formulation and skill assessment. *Continental Shelf Research*, 24(18):2187 – 2214, 2004.
- [41] Y. Zhang and A. M. Baptista. SELFE: A semi-implicit Eulerian-Lagrangian finite-element model for cross-scale ocean circulation. *Ocean Modelling*, 21:71–96, 2008.